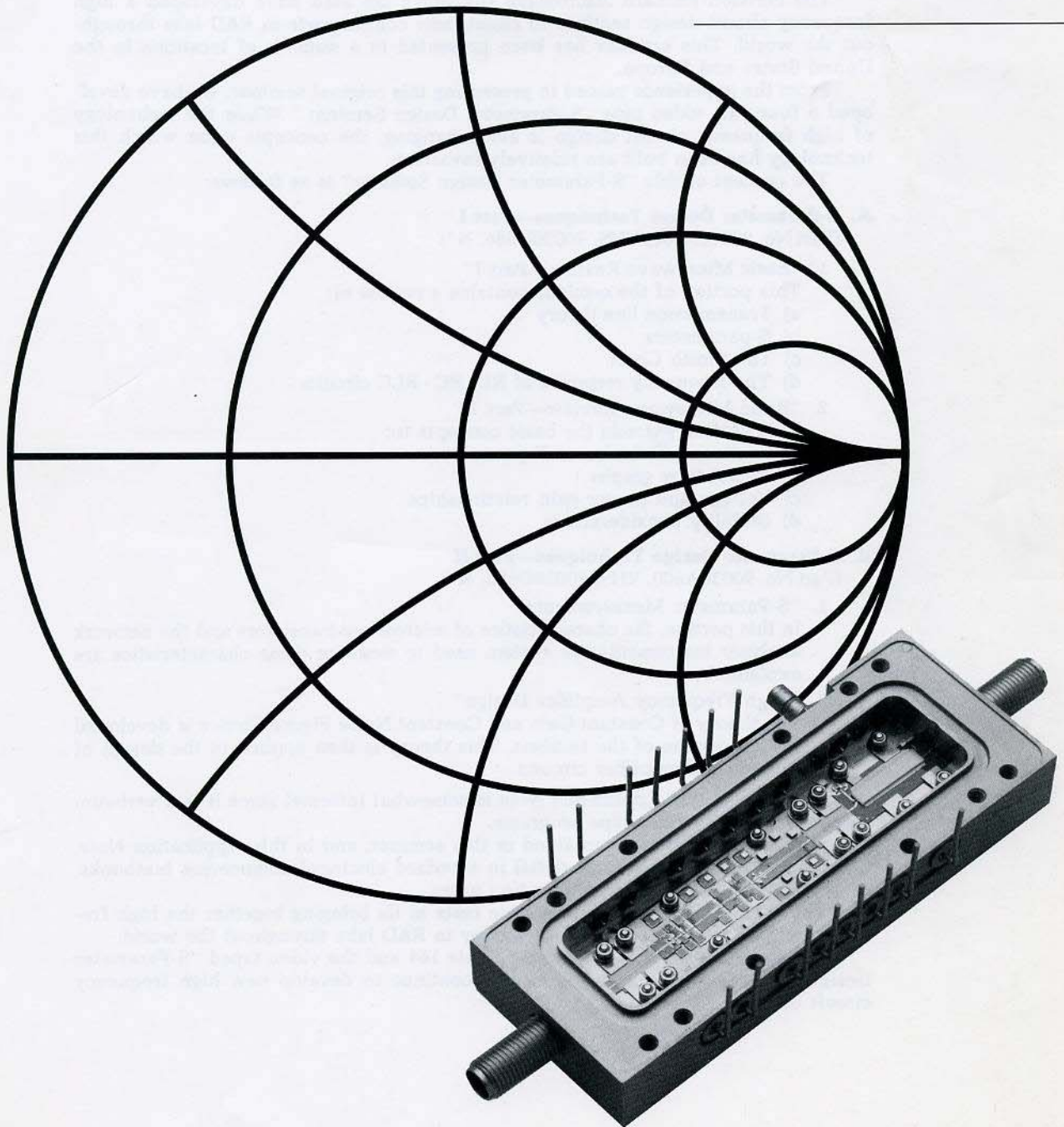


---

# S-Parameter Design

Application Note 154



## S-Parameter Design

### Introduction

The need for new high frequency solid state circuit design techniques has been recognized both by microwave engineers and circuit designers. These engineers are being asked to design solid state circuits that will operate at higher and higher frequencies.

The development of microwave transistors and Hewlett-Packard's network analysis instrumentation systems that permit complete network characterization in the microwave frequency range have greatly assisted these engineers in their work.

The Hewlett-Packard Microwave Division's lab staff have developed a high frequency circuit design seminar to assist their counterparts in R&D labs throughout the world. This seminar has been presented in a number of locations in the United States and Europe.

From the experience gained in presenting this original seminar, we have developed a four-part video tape "S-Parameter Design Seminar." While the technology of high frequency circuit design is ever changing, the concepts upon which this technology has been built are relatively invariant.

The content of this "S-Parameter Design Seminar" is as follows:

#### A. S-Parameter Design Techniques—Part I

(Part No. 90030A586, VHS; 90030D586, ¾")

1. "Basic Microwave Review—Part I"  
This portion of the seminar contains a review of:
  - a) Transmission line theory
  - b) S-parameters
  - c) The Smith Chart
  - d) The frequency response of RL - RC - RLC circuits
2. "Basic Microwave Review—Part II"  
This portion extends the basic concepts to:
  - a) Scattering-Transfer or T-parameters
  - b) Signal flow graphs
  - c) Voltage and power gain relationships
  - d) Stability considerations

#### B. S-Parameter Design Techniques—Part II

(Part No. 90030A600, VHS; 90030D600, ¾")

1. "S-Parameter Measurements"  
In this portion, the characteristics of microwave transistors and the network analyzer instrumentation system used to measure these characteristics are explained.
2. "High Frequency Amplifier Design"  
The theory of Constant Gain and Constant Noise Figure Circles is developed in this portion of the seminar. This theory is then applied in the design of three actual amplifier circuits.

The style of this Application Note is somewhat informal since it is a verbatim transcript of these video tape programs.

Much of the material contained in this seminar, and in this Application Note, has been developed in greater detail in standard electrical engineering textbooks, or in other Hewlett-Packard application notes.

The value of this Application Note rests in its bringing together the high frequency circuit design concepts used today in R&D labs throughout the world.

We are confident that Application Note 154 and the video taped "S-Parameter Design Seminar" will assist you as you continue to develop new high frequency circuit designs.

# Chapter I

## Basic Microwave Review -- I

### Introduction

This first portion of Hewlett-Packard's S-Parameter Design Seminar introduces some fundamental concepts we will use in the analysis and design of high frequency networks.

These concepts are most useful at those frequencies where distributed rather than lumped parameters must be considered. We'll discuss: (1) Scattering or S-parameters, (2) Voltage and power gain relationships as well as (3) Stability criteria for two-port networks in terms of these S-parameters, and (4) Review the Smith Chart.

### Network Characterization

S-parameters are basically a means for characterizing n-port networks. By reviewing some traditional network analysis methods we'll understand why an additional method of network characterization is necessary at higher frequencies.

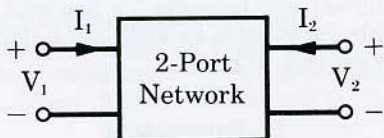


Figure 1

A two-port device (Fig. 1) can be described by a number of parameter sets. We're all familiar with the H, Y, and Z-parameter sets (Fig. 2). All of these network parameters relate total voltages and total currents at each of the two ports. These are the network variables.

#### H-Parameters

$$\begin{aligned} V_1 &= h_{11}I_1 + h_{12}V_2 \\ I_2 &= h_{21}I_1 + h_{22}V_2 \end{aligned}$$

#### Y-Parameters

$$\begin{aligned} I_1 &= y_{11}V_1 + y_{12}V_2 \\ I_2 &= y_{21}V_1 + y_{22}V_2 \end{aligned}$$

#### Z-Parameters

$$\begin{aligned} V_1 &= z_{11}I_1 + z_{12}I_2 \\ V_2 &= z_{21}I_1 + z_{22}I_2 \end{aligned}$$

Figure 2

The only difference in the parameter sets is the choice of independent and dependent variables. The parameters are the constants used to relate these variables.

To see how parameter sets of this type can be determined through measurement, let's focus on the H-parameters.  $H_{11}$  is determined by setting  $V_2$  equal to zero—applying a short circuit to the output port of the network.  $H_{11}$  is then the ratio of  $V_1$  to  $I_1$ —the input impedance of the resulting network.  $H_{12}$  is determined by measuring the ratio of  $V_1$  to  $V_2$ —the reverse voltage gain—with the input port open circuited (Fig. 3). The important thing to note here is that both open and short circuits are essential for making these measurements.

$$h_{11} = \left. \frac{V_1}{I_1} \right|_{V_2=0}$$

$$h_{12} = \left. \frac{V_1}{V_2} \right|_{I_1=0}$$

Figure 3

Moving to higher and higher frequencies, some problems arise:

1. Equipment is not readily available to measure total voltage and total current at the ports of the network.
2. Short and open circuits are difficult to achieve over a broad band of frequencies.
3. Active devices, such as transistors and tunnel diodes, very often will not be short or open circuit stable.

Some method of characterization is necessary to overcome these problems. The logical variables to use at these frequencies are **traveling waves** rather than total voltages and currents.

### Transmission Lines

Let's now investigate the properties of traveling waves. High frequency systems have a source of power. A portion of this power is delivered to a load by means of transmission lines (Fig. 4).

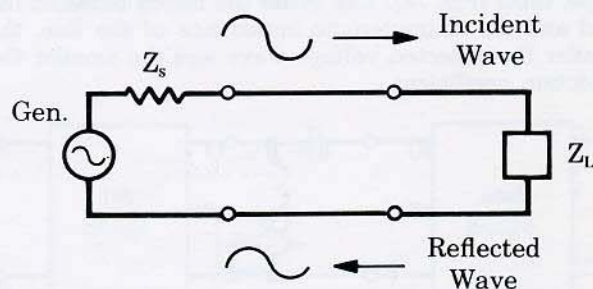
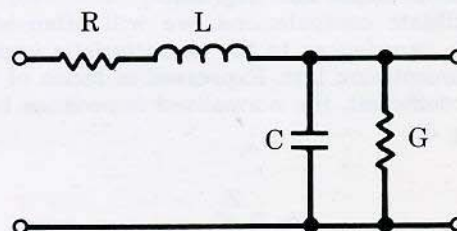


Figure 4

Voltage, current, and power can be considered to be in the form of waves traveling in both directions along this transmission line. A portion of the waves incident on the load will be reflected. It then becomes incident on the source, and in turn re-reflects from the source (if  $Z_s \neq Z_0$ ), resulting in a standing wave on the line.

If this transmission line is uniform in cross section, it can be thought of as having an equivalent series impedance and equivalent shunt admittance per unit length (Fig. 5).



Uniform Transmission Line

Figure 5

A lossless line would simply have a series inductance and a shunt capacitance. The characteristic impedance of the lossless line,  $Z_0$ , is defined as  $Z_0 = \sqrt{L/C}$ . At microwave frequencies, most transmission lines have a 50-ohm characteristic impedance. Other lines of 75, 90, and 300-ohm impedance are often used.

Although the general techniques developed in this seminar may be applied for any characteristic impedance, we will be using lossless 50-ohm transmission lines.

We've seen that the incident and reflected voltages on a transmission line result in a standing voltage wave on the line.

The value of this total **voltage** at a given point along the length of the transmission line is the sum of the incident and reflected waves at that point (Fig. 6a).

$$\begin{aligned} \text{a) } V_t &= E_{inc} + E_{refl}. \\ \text{b) } I_t &= \frac{E_{inc} - E_{refl}}{Z_0} \end{aligned}$$

**Figure 6**

The total **current** on the line is the **difference** between the incident and reflected voltage waves divided by the characteristic impedance of the line (Fig. 6b).

Another very useful relationship is the reflection coefficient,  $\Gamma$ . This is a measure of the quality of the impedance match between the load and the characteristic impedance of the line. The reflection coefficient is a complex quantity having a magnitude,  $\rho$ , and an angle,  $\theta$  (Fig. 7a). The better the match between the load and the characteristic impedance of the line, the smaller the reflected voltage wave and the smaller the reflection coefficient.

$$\begin{aligned} \text{a) } \Gamma &= \rho \angle \theta \\ &= \frac{E_{refl.}}{E_{inc.}} \\ \text{b) } \Gamma &= \frac{Z_L - Z_0}{Z_L + Z_0} \\ &= \frac{Y_0 - Y_L}{Y_0 + Y_L} \end{aligned}$$

**Figure 7**

This can be seen more clearly if we express the reflection coefficient in terms of load impedance or load admittance. The reflection coefficient can be made equal to zero by selecting a load,  $Z_L$ , equal to the characteristic impedance of the line (Fig. 7b).

To facilitate computations, we will often want to normalize impedances to the characteristic impedance of the transmission line. Expressed in terms of the reflection coefficient, the normalized impedance has this form (Fig. 8).

$$\begin{aligned} z_N &= \frac{Z_L}{Z_0} \\ &= \frac{1 + \Gamma}{1 - \Gamma} \end{aligned}$$

**Figure 8**

### S-Parameters

Having briefly reviewed the properties of transmission lines, let's insert a two-port network into the line (Fig. 9). We now have additional traveling waves that are interrelated. Looking at  $E_{r2}$ , we see that it is made up of that portion of  $E_{i2}$  reflected from the output port of the network as well as that portion of  $E_{i1}$  that is transmitted through the network. Each of the other waves are similarly made up of a combination of two waves.

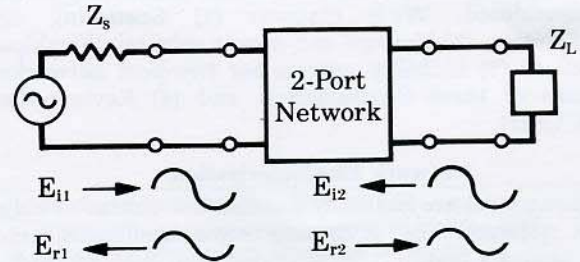


**Figure 9**

It should be possible to relate these four traveling waves by some parameter set. While the derivation of this parameter set will be made for two-port networks, it is applicable for n-ports as well. Let's start with the H-parameter set (Fig. 10).

### H-Parameters

$$\begin{aligned} V_1 &= h_{11}I_1 + h_{12}V_2 \\ I_2 &= h_{21}I_1 + h_{22}V_2 \end{aligned}$$

**Figure 10**

$$\begin{aligned} V_1 &= E_{i1} + E_{r1} & V_2 &= E_{i2} + E_{r2} \\ I_1 &= \frac{E_{i1} - E_{r1}}{Z_0} & I_2 &= \frac{E_{i2} - E_{r2}}{Z_0} \end{aligned}$$

**Figure 11**

By substituting the expressions for total voltage and total current (Fig. 11) on a transmission line into this parameter set, we can rearrange these equations such that the incident traveling voltage waves are the independent variables; and the reflected traveling voltage waves are the dependent variables (Fig. 12).

$$\begin{aligned} E_{r1} &= f_{11}(h) E_{i1} + f_{12}(h) E_{i2} \\ E_{r2} &= f_{21}(h) E_{i1} + f_{22}(h) E_{i2} \end{aligned}$$

**Figure 12**

The functions  $f_{11}$ ,  $f_{21}$  and  $f_{12}$ ,  $f_{22}$  represent a new set of network parameters relating traveling voltage waves rather than total voltages and total currents. In this case these functions are expressed in terms of H-parameters. They could have been derived from any other parameter set.

It is appropriate that we call this new parameter set "scattering parameters," since they relate those waves scattered or reflected from the network to those waves incident upon the network. These scattering parameters will commonly be referred to as S-parameters.

Let's go one step further. If we divide both sides of these equations by  $\sqrt{Z_0}$ , the characteristic impedance of the transmission line, the relationship will not change. It will, however, give us a change in variables (Fig. 13). Let's now define the new variables:

$$a_1 = \frac{E_{i1}}{\sqrt{Z_0}} \quad a_2 = \frac{E_{i2}}{\sqrt{Z_0}}$$

$$b_1 = \frac{E_{r1}}{\sqrt{Z_0}} \quad b_2 = \frac{E_{r2}}{\sqrt{Z_0}}$$

Figure 13

Notice that the square of the magnitude of these new variables has the dimension of power.  $|a_1|^2$  can then be thought of as the incident power on port one.  $|b_1|^2$  as power reflected from port one. These new waves can be called traveling power waves rather than traveling voltage waves. Throughout this seminar, we will simply refer to these waves as **traveling waves**.

Looking at the new set of equations in a little more detail, we see that the S-parameters relate these four waves in this fashion (Fig. 14).

$$b_1 = S_{11} a_1 + S_{12} a_2$$

$$b_2 = S_{21} a_1 + S_{22} a_2$$

Figure 14

### S-Parameter Measurement

We saw how the H-parameters are measured. Let's now see how we go about measuring the S-parameters. For  $S_{11}$ , we terminate the output port of the network and measure the ratio  $b_1$  to  $a_1$  (Fig. 15). Terminating the output port in an impedance equal to the characteristic impedance of the transmission line is equivalent to setting  $a_2 = 0$ , since a traveling wave incident on this load will be totally absorbed.  $S_{11}$  is the input reflection coefficient of the network. Under the same conditions, we can measure  $S_{21}$ , the forward transmission through the network. This is the ratio of  $b_2$  to  $a_1$  (Fig. 16). This could either be the gain of an amplifier or the attenuation of a passive network.

$$S_{11} = \left. \frac{b_1}{a_1} \right|_{a_2=0}$$

Figure 15

$$S_{21} = \left. \frac{b_2}{a_1} \right|_{a_2=0}$$

Figure 16

By terminating the input side of the network, we set  $a_1 = 0$ .  $S_{22}$ , the output reflection coefficient, and  $S_{12}$ , the reverse transmission coefficient, can then be measured (Fig. 17).

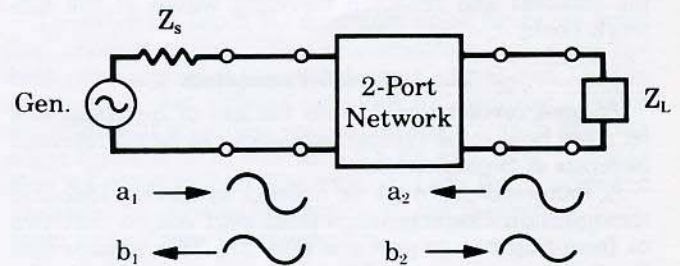
$$S_{22} = \left. \frac{b_2}{a_2} \right|_{a_1=0}$$

$$S_{12} = \left. \frac{b_1}{a_2} \right|_{a_1=0}$$

Figure 17

A question often arises about the terminations used when measuring the S-parameters. Since the transmission line is terminated in the characteristic impedance of the line, does the network port have to be matched to that impedance as well? The answer is no!

To see why, let's look once again at the network enmeshed in the transmission line (Fig. 18). If the load impedance is equal to the characteristic impedance of the line, any wave traveling toward the load would be totally absorbed by the load. It would not reflect back to the network. This sets  $a_2 = 0$ . This condition is completely independent from the network's output impedance.

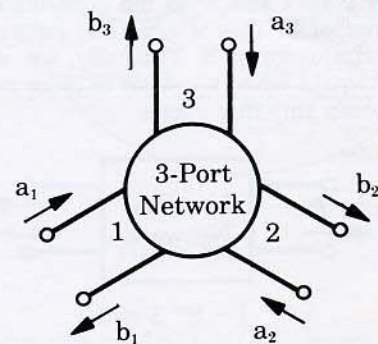


$$\text{If: } Z_L = Z_0, \quad a_2 = 0$$

Figure 18

### Multiple-Port Networks

So far we have just discussed two-port networks. These concepts can be expanded to multiple-port networks. To characterize a three-port network, for example, nine parameters would be required (Fig. 19).  $S_{11}$ , the input reflection coefficient at port one, is measured by terminating the second and third ports with an impedance equal to the characteristic impedance of the line at these ports. This again ensures that  $a_2 = a_3 = 0$ . We could go through the remaining S-parameters and measure them in a similar way, once the other two ports are properly terminated.



$$S_{11} = \left. \frac{b_1}{a_1} \right|_{a_2=a_3=0}$$

Figure 19

What is true for two- and three-port networks is similarly true for n-port networks (Fig. 20). The number of measurements required for characterizing these more complex networks goes up as the square of the number of ports. The concept and method of parameter measurement, however, is the same.

$$\begin{bmatrix} b_1 \\ b_2 \\ \vdots \\ b_N \end{bmatrix} = \begin{bmatrix} S_{11} & S_{12} & \dots & S_{1N} \\ S_{21} & S_{22} & \dots & S_{2N} \\ \vdots & \vdots & \ddots & \vdots \\ S_{N1} & S_{N2} & \dots & S_{NN} \end{bmatrix} \begin{bmatrix} a_1 \\ a_2 \\ \vdots \\ a_N \end{bmatrix}$$

Figure 20

Let's quickly review what we've done up to this point. We started off with a familiar network parameter set relating total voltages and total currents at the ports of the network. We then reviewed some transmission line concepts. Applying these concepts, we derived a new set of parameters for a two-port network relating the incident and reflected traveling waves at the network ports.

**The Use of S-Parameters**

To gain further insight into the use of S-parameters, let's see how some typical networks can be represented in terms of S-parameters.

A **reciprocal network** is defined as having identical transmission characteristics from port one to port two or from port two to port one (Fig. 21). This implies that the S-parameter matrix is equal to its transpose. In the case of a two-port network,  $S_{12} = S_{21}$ .

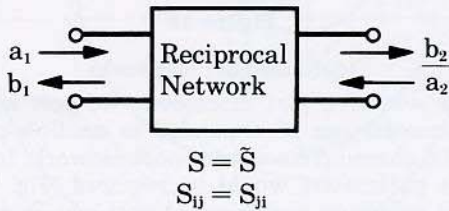


Figure 21

A **lossless network** does not dissipate any power. The power incident on the network must be equal to the power reflected or  $\sum |a_n|^2 = \sum |b_n|^2$  (Fig. 22). In the case of a two-port,  $|a_1|^2 + |a_2|^2 = |b_1|^2 + |b_2|^2$ . This implies that the S-matrix is unitary as defined here. Where: I is the identity matrix and  $S^*$  is the complex conjugate of the transpose of S. This is generally referred to as the hermetian conjugate of S. Typically, we will be using lossless networks when we want to place matching networks between amplifier stages.

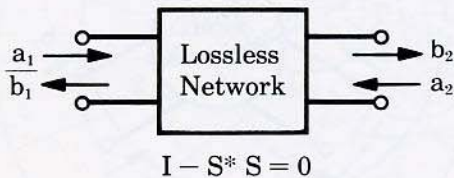


Figure 22

For a **lossy network**, the net power reflected is less than the net incident power (Fig. 23). The difference is the power dissipated in the network. This implies that the statement  $I - S^* S$  is positive definite, or the eigen-

values for this matrix are in the left half plane so that the impulse response of the network is made up of decaying exponentials.

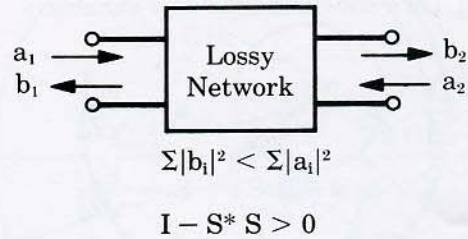


Figure 23

**Change in Reference Plane**

Another useful relationship is the equation for changing reference planes. We often need this in the measurement of transistors and other active devices where, due to device size, it is impractical to attach RF connectors to the actual device terminals.

Imbedding the device in the transmission line structure, we can then measure the S-parameters at these two planes (Fig. 24). We've added a length of line,  $\phi_1$ , to port one of the device and another length,  $\phi_2$ , to port two.

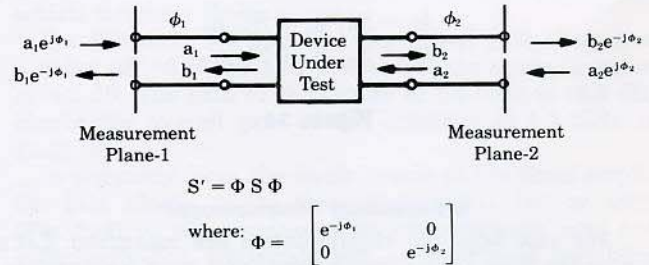


Figure 24

The S-parameter matrix,  $S'$ , measured at these two planes is related to the S-parameter matrix of the device, S, by this expression. We've simply pre-multiplied and post-multiplied the device's S-parameter matrix by the diagonal matrix,  $\Phi$ .

To see what's happening here, let's carry through the multiplication of the  $S_{11}$  term. It will be multiplied by  $e^{-j\phi_1}$  twice, since  $a_1$  travels through this length of line,  $\phi_1$ , and gets reflected and then travels through it again (Fig. 25). The transmission term,  $S'_{21}$ , would have this form, since the input wave,  $a_1$ , travels through  $\phi_1$  and the transmitted wave,  $b_2$ , through  $\phi_2$ . From the measured S-parameters,  $S'$ , we can then determine the S-parameters of the device, S, with this relationship (Fig. 26).

$$S'_{11} = S_{11} e^{-j2\phi_1}$$

$$S'_{21} = S_{21} e^{-j(\phi_1 + \phi_2)}$$

Figure 25

$$S = \Phi^{-1} S' \Phi^{-1}$$

Figure 26

### Analysis of Networks Using S-Parameters

Let's now look at a simple example which will demonstrate how S-parameters can be determined analytically.

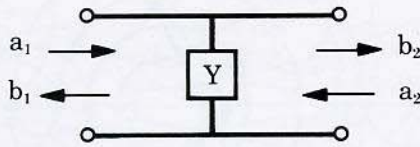


Figure 27

Using a shunt admittance, we see the incident and reflected waves at the two ports (Fig. 27). We first normalize the admittance and terminate the network in the normalized characteristic admittance of the system (Fig. 28a). This sets  $a_2 = 0$ .  $S_{11}$ , the input reflection coefficient of the terminated network, is then: (Fig. 28b).

To calculate  $S_{21}$ , let's recall that the total voltage at the input of a shunt element,  $a_1 + b_1$ , is equal to the total voltage at the output,  $a_2 + b_2$  (Fig. 28c). Since the network is symmetrical and reciprocal,  $S_{22} = S_{11}$  and  $S_{12} = S_{21}$ . We have then determined the four S-parameters for a shunt element.

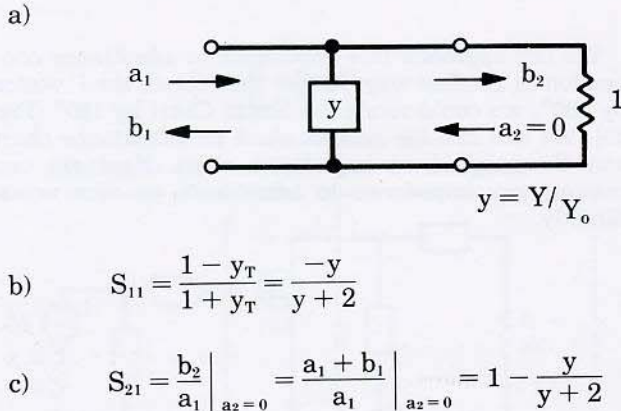


Figure 28

### The Smith Chart

Another basic tool used extensively in amplifier design will now be reviewed. Back in the thirties, Phillip Smith, a Bell Lab engineer, devised a graphical method for solving the oft-repeated equations appearing in microwave theory. Equations like the one for reflection coefficient,  $\Gamma = (Z - 1) / (Z + 1)$ . Since all the values in this equation are complex numbers, the tedious task of solving this expression could be reduced by using Smith's graphical technique. The Smith Chart was a natural name for this technique.

This chart is essentially a mapping between two planes—the Z or impedance plane and the  $\Gamma$  or reflection coefficient plane. We're all familiar with the impedance plane—a rectangular coordinate plane having a real and an imaginary axis. Any impedance can be plotted in this plane. For this discussion, we'll normalize the impedance plane to the characteristic impedance (Fig. 29a).

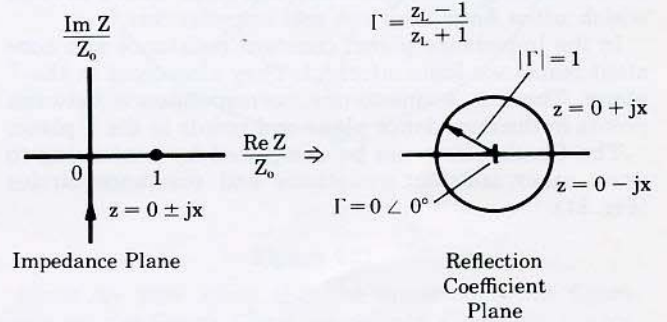
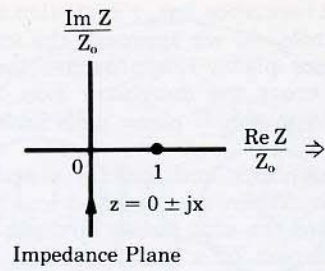


Figure 29

Let's pick out a few values in this normalized plane and see how they map into the  $\Gamma$  plane. Let  $z = 1$ . In a 50-ohm system, this means  $Z = 50$  ohms. For this value,  $|\Gamma| = 0$ , the center of the  $\Gamma$  plane.

We now let  $z$  be purely imaginary; i.e.,  $z = jx$  where  $x$  is allowed to vary from minus infinity to plus infinity. Since  $\Gamma = (jx - 1) / (jx + 1)$ ,  $|\Gamma| = 1$  and its phase angle varies from 0 to 360°. This traces out a circle in the  $\Gamma$  plane (Fig. 29b). For positive reactance,  $jx$  positive, the impedance maps into the upper half circle. For negative reactance, the impedance maps into the lower half circle. The upper region is inductive and the lower region is capacitive.

Now let's look at some other impedance values. A constant resistance line, going through the point  $z = 1$  on the real axis, maps into a circle in the  $\Gamma$  plane. The upper semicircle represents an impedance of  $1 + jx$ , which is inductive; the lower semicircle, an impedance of  $1 - jx$  or capacitive (Fig. 30).

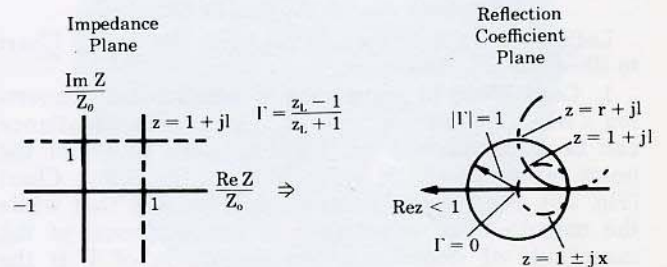


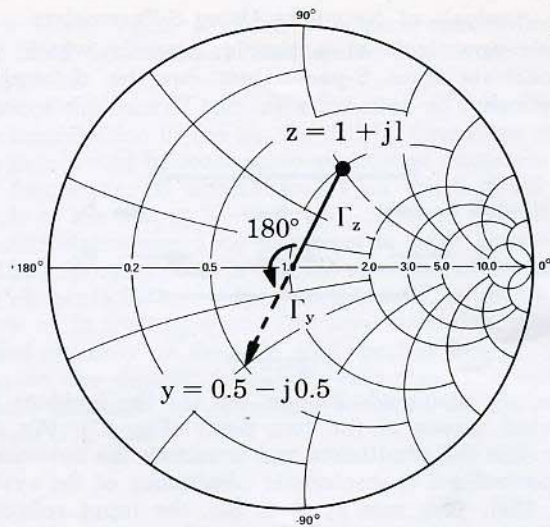
Figure 30

The constant reactance line,  $r + j1$ , also maps into the  $\Gamma$  plane as a circle. As we approach the imaginary axis in the impedance plane,  $\Gamma$  approaches the unit radius circle. As we cross the imaginary axis, the constant reactance circle in the  $\Gamma$  plane goes outside the unit radius circle.

If we now go back and look at  $z$  real, we see at  $z = -1$ ,  $\Gamma = \infty$ . When  $z$  is real and less than one, we move out toward the unit radius circle in the  $\Gamma$  plane. When the real part of  $z$  goes negative,  $\Gamma$  continues along this circle of infinite radius. The entire region outside the unit radius circle represents impedances with negative real parts. We will use this fact later when working with transistors and other active devices which often have negative real impedances.

In the impedance plane, constant resistance and constant reactance lines intersect. They also cross in the  $\Gamma$  plane. There is a one-to-one correspondence between points in the impedance plane and points in the  $\Gamma$  plane.

The Smith Chart can be completed by continuing to draw other constant resistance and reactance circles (Fig. 31).



$$\Gamma_z = \frac{z - 1}{z + 1} \quad \Gamma_y = \frac{1 - y}{1 + y} \quad |y| = \frac{1}{|z|}$$

$$|\Gamma_z| = |\Gamma_y|$$

Figure 32

We can approach this impedance to admittance conversion in another way. Rather than rotate the  $\Gamma$  vector by  $180^\circ$ , we could rotate the Smith Chart by  $180^\circ$  (Fig. 33). We can call the rotated chart an admittance chart and the original an impedance chart. Now we can convert any impedance to admittance, or vice versa, directly.

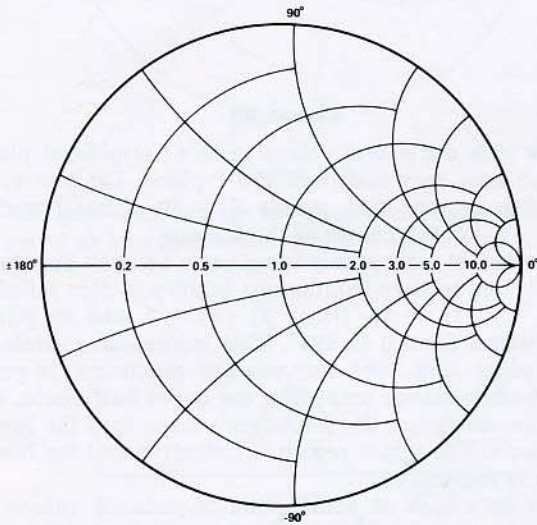


Figure 31

### Applications of the Smith Chart

Let's now try a few examples with the Smith Chart to illustrate its usefulness.

**1. Conversion of impedance to admittance:** Converting a normalized impedance of  $1 + j1$  to an admittance can be accomplished quite easily. Let's first plot the point representing the value of  $z$  on the Smith Chart (Fig. 32). From these relationships, we see that while the magnitude of admittance is the reciprocal of the magnitude of impedance, the magnitude of  $\Gamma$  is the same—but its phase angle is changed by  $180^\circ$ . On the Smith Chart, the  $\Gamma$  vector would rotate through  $180^\circ$ . This point could then be read off as an admittance.

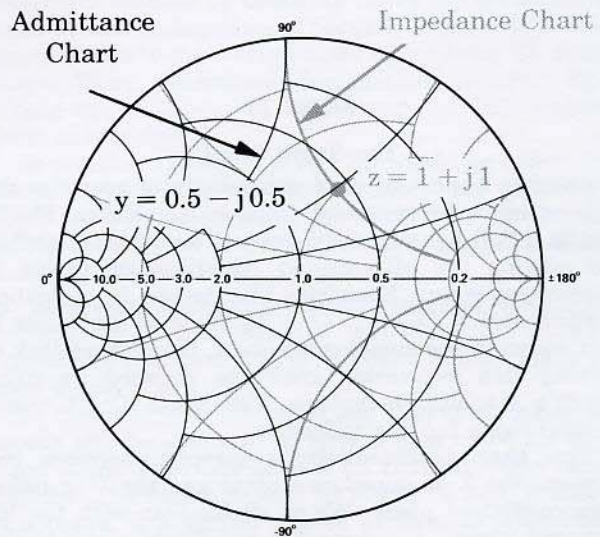


Figure 33



**2. Impedances with negative real parts:** Let's now take a look at impedances with negative real parts. Here again is a conventional Smith Chart defined by the boundary of the unit radius circle. If we have an impedance that is inductive with a negative real part, it would map into the  $\Gamma$  plane outside the chart (Fig. 34). One way to bring this point back onto the chart would be to plot the reciprocal of  $\Gamma$ , rather than  $\Gamma$  itself. This would be inconvenient since the phase angle would not be preserved. What was a map of an inductive impedance appears to be capacitive.

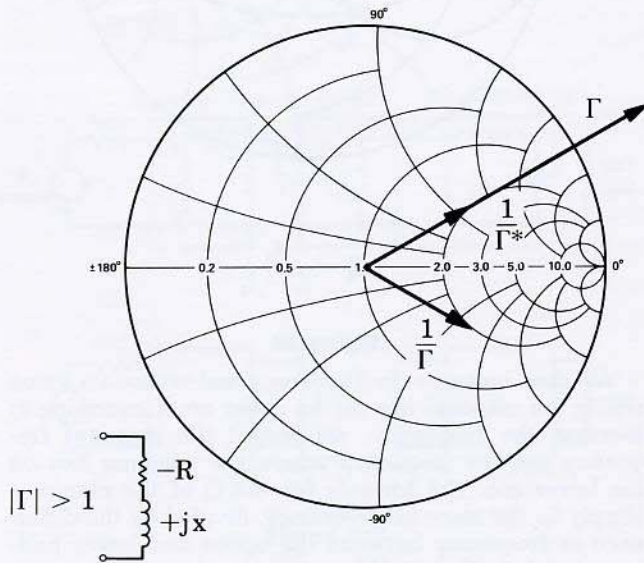


Figure 34

If we plot the reciprocal of the complex conjugate of  $\Gamma$ , however, the phase angle is preserved. This value lies along the same line as the original  $\Gamma$ . Typically in the Hewlett-Packard transistor data sheets, impedances of this type are plotted this way.

There are also compressed Smith Charts available that include the unit radius chart plus a great deal of the negative impedance region. This chart has a radius which corresponds to a reflection coefficient whose magnitude is 3.16 (Fig. 35).

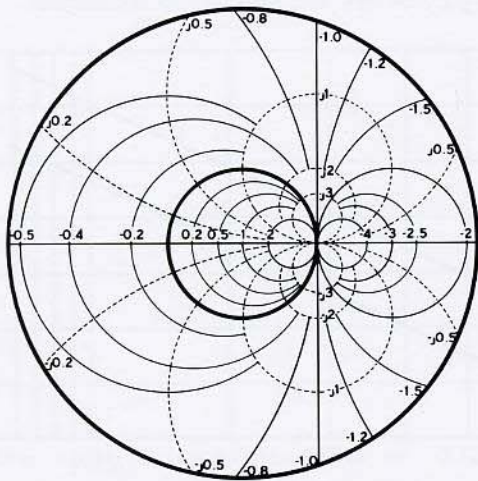


Figure 35

In the rest of this seminar, we will see how easily we can convert measured reflection coefficient data to impedance information by slipping a Smith Chart overlay over the Hewlett-Packard network analyzer polar display.

**3. Frequency response of networks:** One final point needs to be covered in this brief review of the Smith Chart and that is the frequency response for a given network. Let's look at a network having an impedance,  $z = 0.4 + jx$  (Fig. 36). As we increase the frequency of the input signal, the impedance plot for the network moves clockwise along a constant resistance circle whose value is 0.4. This generally clockwise movement with increasing frequency is typical of impedance plots on the Smith Chart for passive networks. This is essentially Foster's Reactance Theorem.

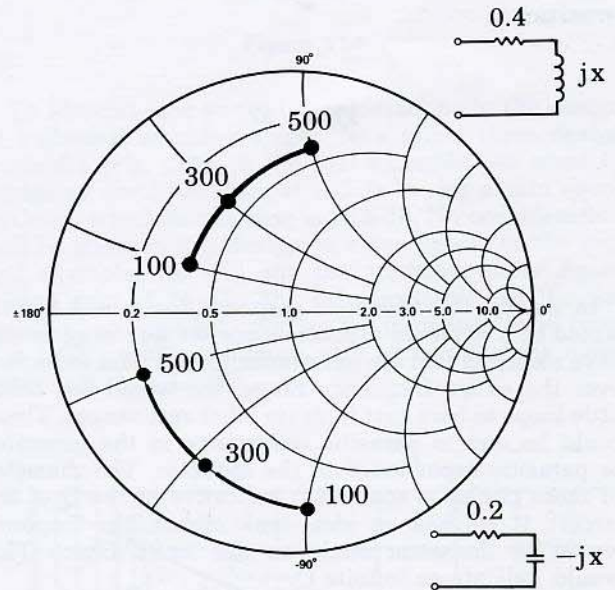


Figure 36

If we now look at another circuit having a real part of 0.2 and an imaginary part that is capacitive, the impedance plot again moves in a clockwise direction with an increase in frequency.

Another circuit that is often encountered is the tank circuit. Here again, the Smith Chart is useful for plotting the frequency response (Fig. 37). For this circuit at zero frequency, the inductor is a short circuit. We start our plot at the point,  $z = 0$ . As the frequency increases, the inductive reactance predominates. We move in a clockwise direction. At resonance, the impedance is purely real, having the value of the resistor. If the resistor had a higher value, the cross-over point at resonance would be farther to the right on the Smith Chart. As the frequency continues to increase, the response moves clockwise into the capacitive region of the Smith Chart until we reach infinite frequency, where the impedance is again zero.

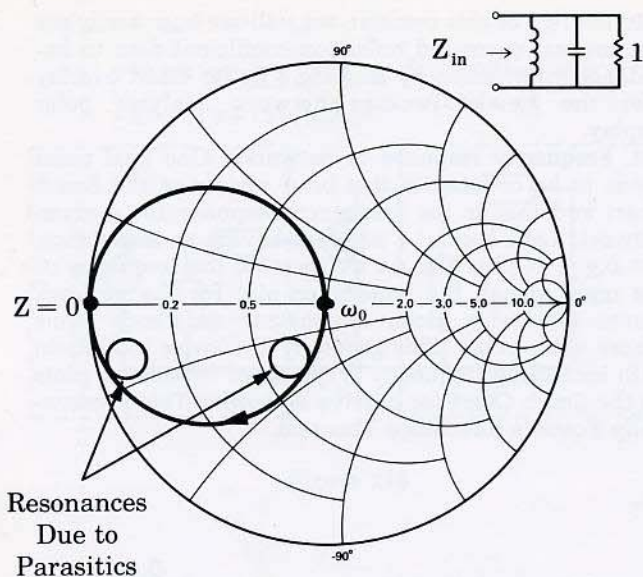
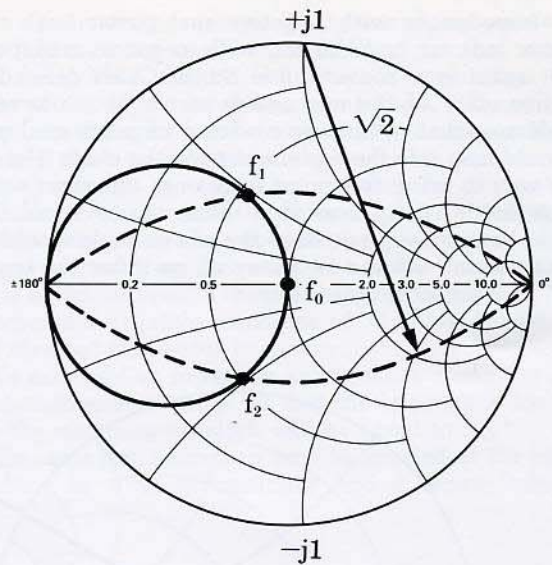


Figure 37

In theory, this complete response for a tank circuit would be a circle. In practice, since we do not generally have elements that are pure capacitors or pure inductors over the entire frequency range, we would see other little loops in here that indicate other resonances. These could be due to parasitic inductance in the capacitor or parasitic capacitance in the inductor. The diameter of these circles is somewhat indicative of the Q of the circuit. If we had an ideal tank circuit, the response would be the outer circle on the Smith Chart. This would indicate an infinite Q.

Hewlett-Packard Application Note 117-1 describes other possible techniques for measuring the Q of cavities and YIG spheres using the Smith Chart. One of these techniques uses the fact that with a tank circuit, the real part of the circuit equals the reactive part at the half-power points. Let's draw two arcs connecting these points on the Smith Chart (Fig. 38). The centers for these arcs are at  $\pm j1$ . The radius of the arcs is  $\sqrt{2}$ .



$$Q = \frac{f_0}{f_2 - f_1}$$

Figure 38

We then increase the frequency and record its value where the response lies on the arc. Continuing to increase the frequency, we record the resonant frequency and the frequency where the response lies on the lower arc. The formula for the Q of the circuit is simply  $f_0$ , the resonant frequency, divided by the difference in frequency between the upper and lower half-power points.  $Q = f_0/\Delta f$ .

### Summary

Let's quickly review what we've seen with the Smith Chart. It is a mapping of the impedance plane and the reflection coefficient or  $\Gamma$  plane. We discovered that impedances with positive real parts map inside the unit radius circle on the Smith Chart. Impedances with negative real parts map outside this unit radius circle. Impedances having positive real parts and inductive reactance map into the upper half of the Smith Chart. Those with capacitive reactance map into the lower half.

In the next part of this S-Parameter Design Seminar, we will continue our discussion of network analysis using S-parameters and flow graph techniques.

## Chapter II

### Basic Microwave Review -- II

This second portion of Hewlett-Packard's Basic Microwave Review will introduce some additional concepts that are used in high frequency amplifier design.

#### Scattering Transfer Parameters

Let's now proceed to a set of network parameters used when cascading networks. We recall that we developed the S-parameters by defining the reflected waves as dependent variables, and incident waves as independent variables (Fig. 39a). We now want to rearrange these equations such that the input waves  $a_1$  and  $b_1$  are the dependent variables and the output waves  $a_2$  and  $b_2$  the independent variables. We'll call this new parameter set scattering transfer parameters or T-parameters (Fig. 39b).

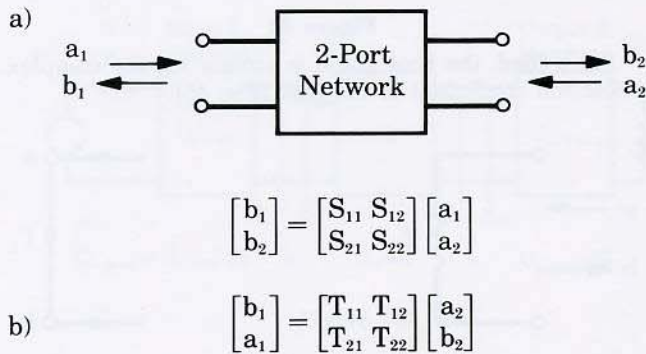


Figure 39

The T-parameters can be developed by manipulating the S-parameter equations into the appropriate form. Notice that the denominator of each of these terms is  $S_{21}$  (Fig. 40).

$$\begin{bmatrix} T_{11} & T_{12} \\ T_{21} & T_{22} \end{bmatrix} = \begin{bmatrix} -\frac{S_{11}S_{22} - S_{12}S_{21}}{S_{21}} & \frac{S_{11}}{S_{21}} \\ -\frac{S_{22}}{S_{21}} & \frac{1}{S_{21}} \end{bmatrix}$$

$$\begin{bmatrix} S_{11} & S_{12} \\ S_{21} & S_{22} \end{bmatrix} = \begin{bmatrix} \frac{T_{12}}{T_{22}} & \frac{T_{11}T_{22} - T_{12}T_{21}}{T_{22}} \\ \frac{1}{T_{22}} & -\frac{T_{21}}{T_{22}} \end{bmatrix}$$

Figure 40

We can also find the S-parameters as a function of the T-parameters.

While we defined the T-parameters in a particular way, we could have defined them such that the **output** waves are the dependent variables and the **input** waves are the independent variables. This alternate definition can result in some problems when designing with active unilateral devices (Fig. 41).

$$[T_A] = \begin{bmatrix} \frac{S_{12}S_{21} - S_{11}S_{22}}{S_{12}} & \frac{S_{22}}{S_{12}} \\ -\frac{S_{11}}{S_{12}} & \frac{1}{S_{12}} \end{bmatrix}$$

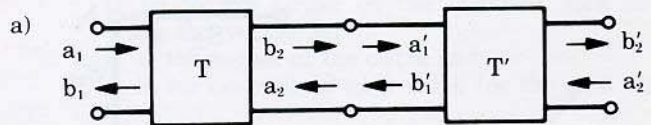
Figure 41

Using the alternate definition for the transfer parameters, the denominator in each of these terms is  $S_{12}$  rather than  $S_{21}$  as we saw earlier.

Working with amplifiers, we often assume the device to be unilateral, or  $S_{12} = 0$ . This would cause this alternate T-parameter set to go to infinity.

Both of these definitions for T-parameters can be encountered in practice. In general, we prefer to define the T-parameters with the output waves as the dependent variables, and the input waves as the independent variables.

We use this new set of transfer parameters when we want to cascade networks—two stages of an amplifier, or an amplifier with a matching network for example (Fig. 42a). From measured S-parameter data, we can define the T-parameters for the two networks. Since the output waves of the first network are identical to the input waves of the second network, we can now simply multiply the two T-parameter matrices and arrive at a set of equations for the overall network (Fig. 42b).



b) 
$$\begin{bmatrix} b_1 \\ a_1 \end{bmatrix} = \begin{bmatrix} T_{11} & T_{12} \\ T_{21} & T_{22} \end{bmatrix} \begin{bmatrix} a_2 \\ b_2 \end{bmatrix} \text{ and } \begin{bmatrix} b'_1 \\ a'_1 \end{bmatrix} = \begin{bmatrix} T'_{11} & T'_{12} \\ T'_{21} & T'_{22} \end{bmatrix} \begin{bmatrix} a'_2 \\ b'_2 \end{bmatrix}$$

but 
$$\begin{bmatrix} a_2 \\ b_2 \end{bmatrix} = \begin{bmatrix} b'_1 \\ a'_1 \end{bmatrix}$$

Therefore 
$$\begin{bmatrix} b_1 \\ a_1 \end{bmatrix} = \begin{bmatrix} T_{11} & T_{12} \\ T_{21} & T_{22} \end{bmatrix} \begin{bmatrix} T'_{11} & T'_{12} \\ T'_{21} & T'_{22} \end{bmatrix} \begin{bmatrix} a'_2 \\ b'_2 \end{bmatrix}$$

Figure 42

Since matrix multiplication is, in general, not commutative, these T-parameter matrices must be multiplied in the proper order. When cascading networks, we'll have to multiply the matrices in the same order as the networks are connected. Using the alternate definition for T-parameters, previously described, this matrix multiplication must be done in reverse order.

This transfer parameter set becomes very useful when using computer-aided design techniques where matrix multiplication is an easy task.

## Signal Flow Graphs

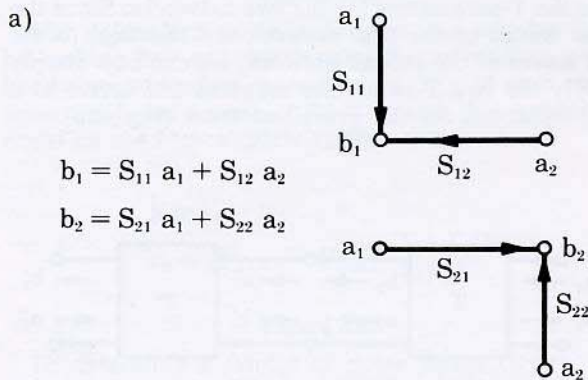
If we design manually, however, we can use still another technique—signal flow graphs—to follow incident and reflected waves through the networks. This is a comparatively new technique for microwave network analysis.

### A. Rules

We'll follow certain rules when we build up a network flow graph.

1. Each variable,  $a_1$ ,  $a_2$ ,  $b_1$ , and  $b_2$  will be designated as a node.
2. Each of the S-parameters will be a branch.
3. Branches enter dependent variable nodes, and emanate from the independent variable nodes.
4. In our S-parameter equations, the reflected waves  $b_1$  and  $b_2$  are the dependent variables and the incident waves  $a_1$  and  $a_2$  are the independent variables.
5. Each node is equal to the sum of the branches entering it.

Let's now apply these rules to the two S-parameter equations (Fig. 43a). The first equation has three nodes— $b_1$ ,  $a_1$ , and  $a_2$ .  $b_1$  is a dependent node and is connected to  $a_1$  through the branch  $S_{11}$  and to node  $a_2$  through the branch  $S_{12}$ . The second equation is constructed similarly. We can now overlay these to have a complete flow graph for a two-port network (Fig. 43b).



b) Complete Flow Graph for 2-Port

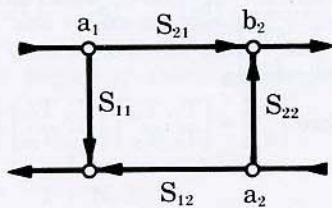


Figure 43

The relationship between the traveling waves is now easily seen. We have  $a_1$  incident on the network. Part of it transmits through the network to become part of  $b_2$ . Part of it is reflected to become part of  $b_1$ . Meanwhile, the  $a_2$  wave entering port two is transmitted through the network to become part of  $b_1$  as well as being reflected from port two as part of  $b_2$ . By merely following the arrows, we can tell what's going on in the network.

This technique will be all the more useful as we cascade networks or add feedback paths.

### B. Application of Flow Graphs

Let's now look at several typical networks we will encounter in amplifier designs. A **generator** with some internal voltage source and an internal impedance will have a wave emanating from it. The flow graph for the generator introduces a new term,  $b_s$  (Fig. 44). It's defined by the impedance of the generator. The units in this equation look peculiar, but we have to remember that we originally normalized the traveling waves to  $\sqrt{Z_0}$ . The magnitude of  $b_s$ , squared then has the dimension of power.

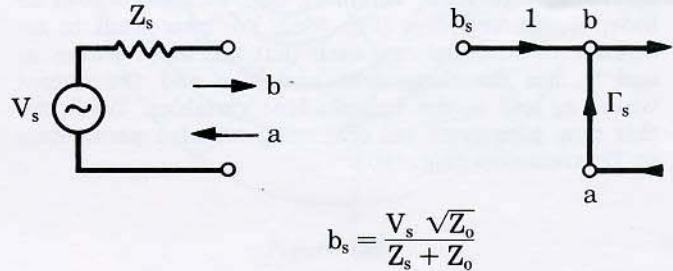


Figure 44

For a **load**, the flow graph is simply  $\Gamma_L$ , the complex reflection coefficient of the load (Fig. 45).

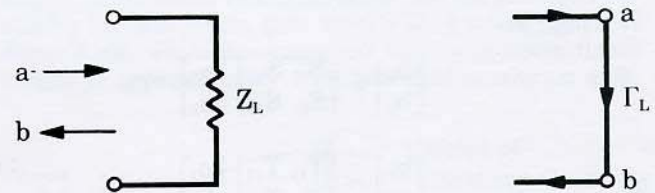


Figure 45

When the load is connected to the generator, we see a wave emanating from the generator incident on the load and a wave reflected back to the generator from the load (Fig. 46).

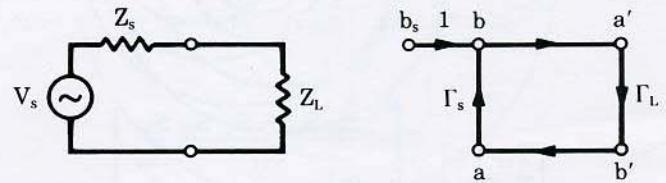


Figure 46

To demonstrate the utility of flow graphs, let's embed a two-port network between a source and a load. Combining the examples we have seen, we can now draw a flow graph for the system (Fig. 47).

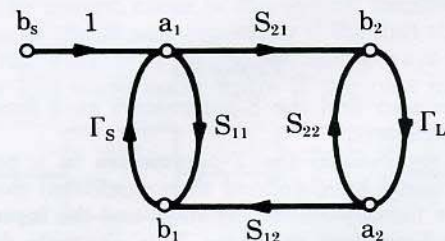


Figure 47

We can now apply the rule known as Mason's rule—or as it is often called, the non-touching loop rule—to solve for the value of any node in this network. Before applying the rule, however, we must first define several additional terms.

A **first order loop** is defined as the product of the branches encountered in a journey starting from a node and moving in the direction of the arrows back to that original node. To illustrate this, let's start at node  $a_1$ . One first order loop is  $S_{11}\Gamma_s$ . Another first order loop is  $S_{21}\Gamma_L S_{12}\Gamma_s$ . If we now start at node  $a_2$ , we find a third first order loop— $S_{22}\Gamma_L$ . Any of the other loops we encounter is one of these three first order loops.

A **second order loop** is defined as the product of any two non-touching first order loops. Of the three first order loops just found, only  $S_{11}\Gamma_s$  and  $S_{22}\Gamma_L$  do not touch in any way. The product of these two loops establishes the second order loop for this network. More complicated networks involving feedback paths, for example, might have several second order loops.

A **third order loop** is the product of any three non-touching first order loops. This example does not have any third order loops but again more complicated networks would have third order loops and even higher order loops.

Let's now suppose that we are interested in the value of  $b_1$ . In this example,  $b_s$  is the only independent variable since its value will determine the value of each of the other variables in the network.  $B_1$ , therefore, will be a function of  $b_s$ . To determine  $b_1$ , we first have to identify the paths leading from  $b_s$  to  $b_1$ . Following the arrows, we see two paths—(1)  $S_{11}$  and (2)  $S_{21}\Gamma_L S_{12}$ .

The next step is to find the non-touching loops with respect to the paths just found. Here, the path  $S_{11}$  and the first order loop,  $S_{22}\Gamma_L$ , have no nodes or branches in common. With this condition met, we can call  $S_{22}\Gamma_L$  a non-touching loop with respect to the path  $S_{11}$ .

The other path,  $S_{21}\Gamma_L S_{12}$ , touches all of the network's first order loops, hence there are no non-touching loops with respect to this path. Again, in more complex networks, there would be higher order non-touching loops.

Let's now look at the non-touching loop rule itself (Fig. 48). This equation appears to be rather ominous at first glance, but once we go through it term by term, it will be less awesome. This rule determines the ratio of two variables, a dependent to an independent variable. (In our example, we are interested in the ratio  $b_1$  to  $b_s$ .)

$$T = \frac{P_1[1 - \Sigma L(1)^{(1)} + \Sigma L(2)^{(1)} - \dots] + P_2[1 - \Sigma L(1)^{(2)} \dots]}{1 - \Sigma L(1) + \Sigma L(2) - \Sigma L(3) + \dots}$$

$$T = \frac{b_1}{b_s}$$

Figure 48

$P_1, P_2$ , etc., are the various paths connecting these variables.

This term,  $\Sigma L(1)^{(1)}$ , is the sum of all first order loops that do not touch the first path between the variables.

This term,  $\Sigma L(2)^{(1)}$ , is the sum of all second order loops that do not touch that path, and so on down the line.

Now, this term,  $\Sigma L(1)^{(2)}$ , is the sum of all first order loops that do not touch the second path.

The denominator in this expression is a function of the network geometry. It is simply one minus the sum of all first order loops, plus the sum of all second order loops, minus the third order loops, and so on.

Let's now apply this non-touching loop rule to our network (Fig. 49). The ratio of  $b_1$ , the dependent variable, to  $b_s$ , the independent variable, is equal to the first path,  $S_{11}$ , multiplied by one minus the non-touching first order loop with respect to this path,  $\Gamma_L S_{22}$ .

$$\frac{b_1}{b_s} = \frac{S_{11}(1 - \Gamma_L S_{22}) + S_{21}\Gamma_L S_{12}(1)}{1 - (S_{11}\Gamma_s + S_{22}\Gamma_L + S_{21}\Gamma_L S_{12}\Gamma_s) + S_{11}\Gamma_s S_{22}\Gamma_L}$$

Figure 49

The second path,  $S_{21}\Gamma_L S_{12}$ , is simply multiplied by one since there are no non-touching loops with respect to this path.

The denominator is one minus the sum of first order loops plus the second order loop.

This concludes our example. With a little experience drawing flow graphs of complex networks, you can see how this technique will facilitate your network analysis. In fact, using the flow graph technique, we can now derive several expressions for power and gain that are of interest to the circuit designer.

First of all, we need to know the **power delivered to a load**. We remember that the square of the magnitudes of the incident and reflected waves has the dimension of power. The power delivered to a load is then the difference between the incident power and the reflected power,  $P_{del} = |a|^2 - |b|^2$ .

The **power available from a source** is that power delivered to a conjugately matched load. This implies that the reflection coefficient of the load is the conjugate of the source reflection coefficient— $\Gamma_s^* = \Gamma_L$ .

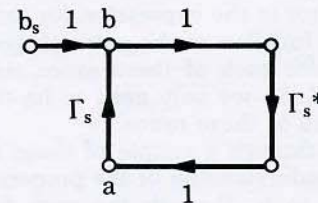


Figure 50

Looking at the flow graph describing these conditions (Fig. 50), we see that the power available from the source is:

$$P_{avs} = |b|^2 - |a|^2$$

Using the flow graph techniques previously described, we see that:

$$b = \frac{b_s}{1 - \Gamma_s \Gamma_s^*} \quad \text{and} \quad a = \frac{b_s \Gamma_s^*}{1 - \Gamma_s \Gamma_s^*}$$

The power available from the source reduces to (Fig. 51):

$$P_{avs} = \frac{|b_s|^2}{1 - |\Gamma_s|^2}$$

Figure 51

We can also develop voltage and power gain equations that will be useful in our amplifier designs using these flow graph techniques. For a two-port network, the **voltage gain** is equal to the total voltage at the output divided by the total voltage at the input,

$$A_v = \frac{a_2 + b_2}{a_1 + b_1}$$

If we divide the numerator and denominator by  $b_s$ , we can relate each of the dependent variables of the system to the one independent variable (Fig. 52a). Now we have four expressions or four ratios that we can determine from the non-touching loop rule.

$$a) \quad A_v = \frac{\frac{a_2}{b_s} + \frac{b_2}{b_s}}{\frac{a_1}{b_s} + \frac{b_1}{b_s}} = \frac{S_{21}\Gamma_L + S_{21}}{1(1 - S_{22}\Gamma_L) + S_{11}(1 - S_{22}\Gamma_L) + S_{21}\Gamma_L S_{12}}$$

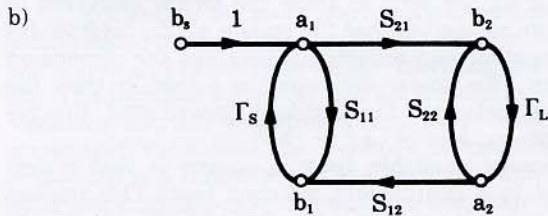


Figure 52

We can simplify this derivation by remembering that the denominator in the expression for the non-touching loop rule is a function of the network geometry. It will be the same for each of these ratios, and will cancel out in the end. So we only need to be concerned with the numerators of these ratios.

Let's trace through a couple of these expressions to firm up our understanding of the process (Fig. 52b).  $A_2$  is connected to  $b_s$  through the path  $S_{21}\Gamma_L$ . All first order loops touch this path, so this path is simply multiplied by one.  $B_2$  is connected to  $b_s$  through the path  $S_{21}$ . All first order loops also touch this path.  $A_1$  is connected to  $b_s$  directly, and there is one non-touching loop,  $S_{22}\Gamma_L$ . We have already determined the ratio of  $b_1$  to  $b_s$ , so we can simply write down the numerator of that expression. We have now derived the voltage gain of the two-port network.

The last expression we wish to develop is that for **transducer power gain**. This will be very important in the amplifier design examples contained in the final section of this seminar. Transducer power gain is defined as the power delivered to a load divided by the power available from a source.

$$G_t = \frac{P_{del}}{P_{avs}}$$

We have already derived these two expressions.

$$G_t = \frac{|b_2|^2 (1 - |\Gamma_L|^2)}{|b_s|^2 / (1 - |\Gamma_s|^2)}$$

What remains is to solve the ratio  $b_2$  to  $b_s$  (Fig. 53a). The only path connecting  $b_s$  and  $b_2$  is  $S_{21}$ . There are no non-touching loops with respect to this path. The denominator is the same as in the previous example: one minus the first order loops plus the second order loop. Taking the magnitude of this ratio, squaring and substituting the result yields the expression for transducer power gain of a two-port network (Fig. 53b).

$$a) \quad \frac{b_2}{b_s} = \frac{S_{21}}{1 - S_{11}\Gamma_s - S_{22}\Gamma_L - S_{21}S_{12}\Gamma_L\Gamma_s + S_{11}\Gamma_s S_{22}\Gamma_L}$$

$$b) \quad G_T = \frac{|S_{21}|^2 (1 - |\Gamma_s|^2) (1 - |\Gamma_L|^2)}{|(1 - S_{11}\Gamma_s)(1 - S_{22}\Gamma_L) - S_{21}S_{12}\Gamma_L\Gamma_s|^2}$$

Figure 53

Needless to say, this is not a simple relationship since the terms are generally complex quantities. Calculator or computer routines will greatly facilitate the circuit designer's task.

Later, when designing amplifiers, we will see that we can simplify this expression by assuming that the amplifier is a unilateral device or  $S_{12} = 0$ . In general, however, this assumption cannot be made and we will be forced to deal with this expression.

One of the things you might want to do is to optimize or maximize the transducer gain of the network. Since the S-parameters at one frequency are constants depending on the device selected and the bias conditions, we have to turn our attention to the source and load reflection coefficients.

### Stability Considerations

To maximize the transducer gain, we must conjugately match the input and the output. Before we do this, we will have to look at what might happen to the network in terms of stability—will the amplifier oscillate with certain values of impedance used in the matching process?

There are two traditional expressions used when speaking of stability: conditional and unconditional stability.

A network is **conditionally stable** if the real part of  $Z_{in}$  and  $Z_{out}$  is greater than zero for **some** positive real source and load impedances at a specific frequency.

A network is **unconditionally stable** if the real part of  $Z_{in}$  and  $Z_{out}$  is greater than zero for **all** positive real source and load impedances at a specific frequency.

It is important to note that these two conditions apply only at **one** specific frequency. The conditions we will now discuss will have to be investigated at many frequencies to ensure broadband stability. Going back to our Smith Chart discussion, we recall that positive real source and load impedances implies:

$$|\Gamma_s| \text{ and } |\Gamma_L| \leq 1$$

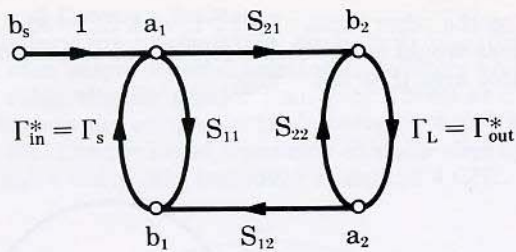


Figure 54

Let's look first at the condition where we want to conjugately match the network to the load and source to achieve maximum transducer gain (Fig. 54). Under these conditions, we can say that the network will be stable if this factor,  $K$ , is greater than one (Fig. 55). Conjugately matched conditions mean that the reflection coefficient of the source,  $\Gamma_s$ , is equal to the conjugate of the input reflection coefficient,  $\Gamma_{in}$

$$\Gamma_s = \Gamma_{in}^*$$

$\Gamma_L$  is equal to the conjugate of the output reflection coefficient,  $\Gamma_{out}$

$$\Gamma_L = \Gamma_{out}^*$$

$$K = \frac{1 + |S_{11}S_{22} - S_{12}S_{21}|^2 - |S_{11}|^2 - |S_{22}|^2}{2|S_{12}||S_{21}|} > 1$$

Figure 55

A **precaution** must be mentioned here. The  $K$  factor must not be considered alone. If we were operating under matched conditions in order to achieve maximum gain, we have to ask ourselves: (1) What effect would temperature changes or drifting S-parameters of the transistor have on the stability of the amplifier? (2) We would also have to be concerned with the effect on stability as we substitute transistors into the circuit. (3) Would these changing conditions affect the conjugate match or the stability of the amplifier? Therefore, we really need to consider these other conditions in addition to the  $K$  factor.

Looking at the input and output reflection coefficient equations, we see a similarity of form (Fig. 56). The only difference is that  $S_{11}$  replaces  $S_{22}$  and  $\Gamma_L$  replaces  $\Gamma_s$ .

$$\Gamma_{in} = \frac{b_1}{a_1} = S_{11} + \frac{S_{21}S_{12}\Gamma_L}{1 - S_{22}\Gamma_L}$$

$$\Gamma_{out} = \frac{b_2}{a_2} = S_{22} + \frac{S_{21}S_{12}\Gamma_s}{1 - S_{11}\Gamma_s}$$

Figure 56

If we set this equation,  $|\Gamma_{in}|$ , equal to one, a boundary would be established. On one side of the boundary, we would expect

$$|\Gamma_{in}| < 1$$

On the other side, we would expect

$$|\Gamma_{in}| > 1$$

Let's first find the boundary by solving this expression (Fig. 57). We insert the real and imaginary values for the S-parameters and solve for  $\Gamma_L$ .

$$|\Gamma_{in}| = \left| S_{11} + \frac{S_{21}S_{12}\Gamma_L}{1 - S_{22}\Gamma_L} \right| = 1$$

Figure 57

The solutions for  $\Gamma_L$  will lie on a circle. The radius of the circle will be given by this expression as a function of S-parameters (Fig. 58a).

a) 
$$\text{radius} = r_L = \left| \frac{S_{12}S_{21}}{|S_{22}|^2 - |\Delta|^2} \right|$$

b) 
$$\text{center} = C_L = \frac{(S_{22} - \Delta S_{11}^*)^*}{|S_{22}|^2 - |\Delta|^2}$$

where:  $\Delta = S_{11}S_{22} - S_{12}S_{21}$

Figure 58

The center of the circle will have this form (Fig. 58b). Having measured the S-parameters of a two-port device at one frequency, we can calculate these quantities.

If we now plot these values on a Smith Chart, we can determine the locus of all values of  $\Gamma_L$  that make  $|\Gamma_{in}| = 1$

This circle then represents the boundary (Fig. 59). The area either inside or outside the circle will represent a stable operating condition.

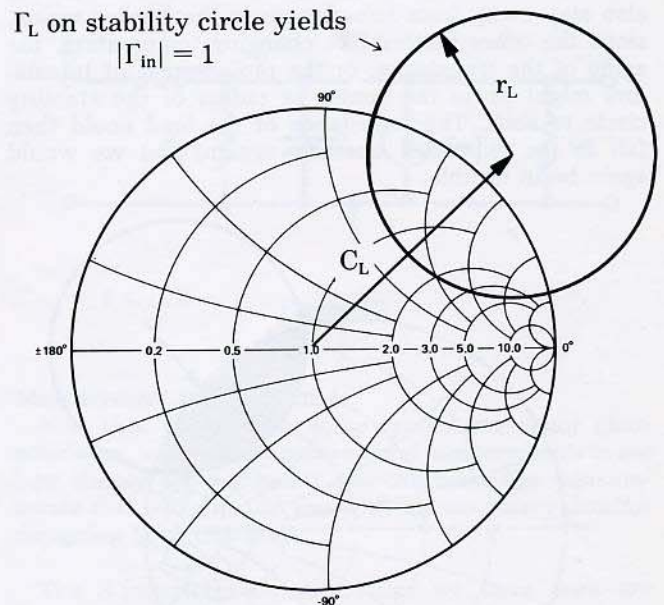


Figure 59

To determine which area represents this stable operating condition, let's make  $Z_L = 50$  ohms, or  $\Gamma_L = 0$ . This represents the point at the center of the Smith Chart. Under these conditions,

$$|\Gamma_{in}| = |S_{11}|$$

Let's now assume that  $S_{11}$  has been measured and its magnitude is less than one.  $\Gamma_{in}$ 's magnitude is also less than one. This means that this point,  $\Gamma_L = 0$ , represents a stable operating condition. This region (Fig. 60) then represents the stable operating condition for the entire network.

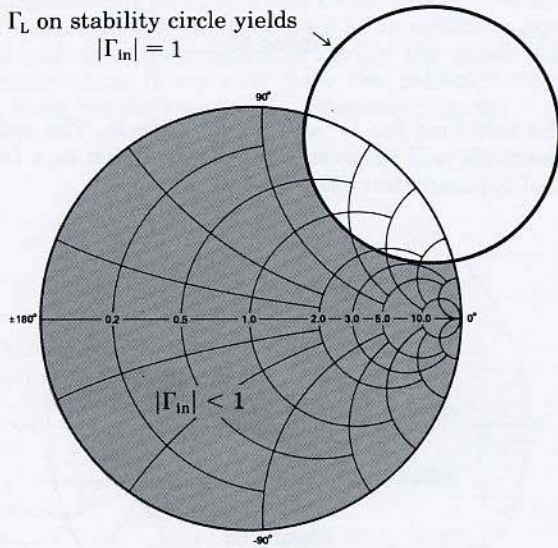


Figure 60

If we select another value of  $\Gamma_L$  that falls **inside** the stability circle, we would have an input reflection coefficient that would be greater than one and the network would be potentially unstable.

If we only deal with passive loads, that is, loads having a reflection coefficient less than or equal to one, then we only have to stay away from those  $\Gamma_L$ 's that are in this region (Fig. 61) to ensure stable operation for the amplifier we are designing. Chances are, we should also stay away from impedances in the border region, since the other factors like changing temperature, the aging of the transistors, or the replacement of transistors might cause the center or radius of the stability circle to shift. The impedance of the load could then fall in the expanded unstable region, and we would again be in trouble.

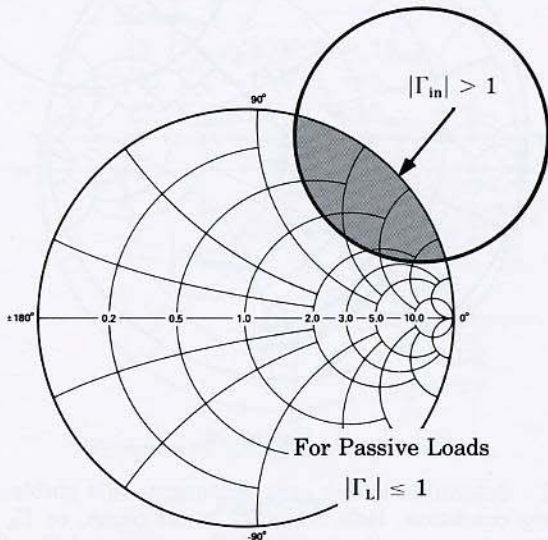


Figure 61

If, on the other hand,  $|S_{11}| > 1$ , with  $Z_{i1} = 50 \Omega$ , then this area would be the stable region and this region the unstable area (Fig. 62).

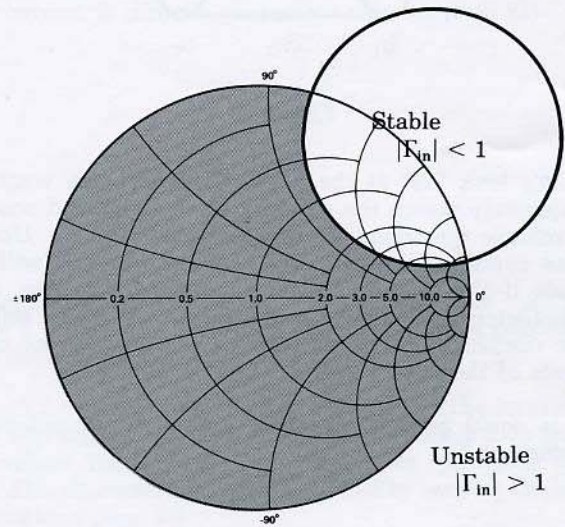


Figure 62

To ensure that we have an **unconditionally stable** condition at a given frequency in our amplifier design, we must be able to place any passive load on the network and drive it with any source impedance without moving into an unstable condition.

From a graphical point of view, we want to be sure that the stability circle falls completely outside the Smith Chart, and we want to make sure that the inside of the stability circle represents the unstable region (Fig. 63). The area outside the stability circle, including the Smith Chart, would then represent the stable operating region.

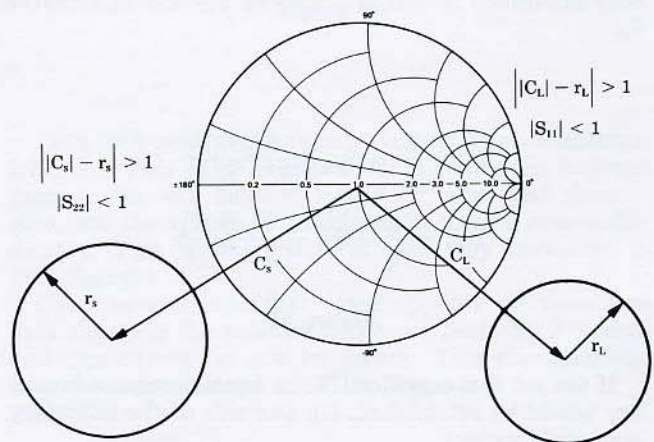


Figure 63



To satisfy this requirement, we must ensure that the magnitude of the vector,  $C_L$ , the distance from the center of the Smith Chart to the center of the stability circle, minus the radius of the stability circle,  $r_L$ , is greater than one. This means that the closest point on the stability circle would be outside the unit radius circle or Smith Chart.

To ensure that the region inside the Smith Chart represents the stable operating condition, the input or output impedance of the network must have a real part greater than zero when the network is terminated in 50 ohms. For completeness, we must also add the output stability circle to gain a better understanding of this concept. This means that the magnitude of  $S_{11}$  and  $S_{22}$  must be less than one.

One word of **caution** about stability.

S-parameters are typically measured at some particular frequency. The stability circles are drawn for **that** frequency. We can be sure that the amplifier will be stable at that frequency, but will it oscillate at some other frequency either inside or outside the frequency range of the amplifier?

Typically, we want to investigate stability over a broad range of frequencies and construct stability circles wherever we might suspect a problem. Shown here are the stability circles drawn for three different frequencies (Fig. 64). To ensure stability between  $f_1$  and  $f_3$ , we stay away from impedances in this (shaded) area. While this process may sound tedious, we do have some notion based on experience where something may get us into trouble.

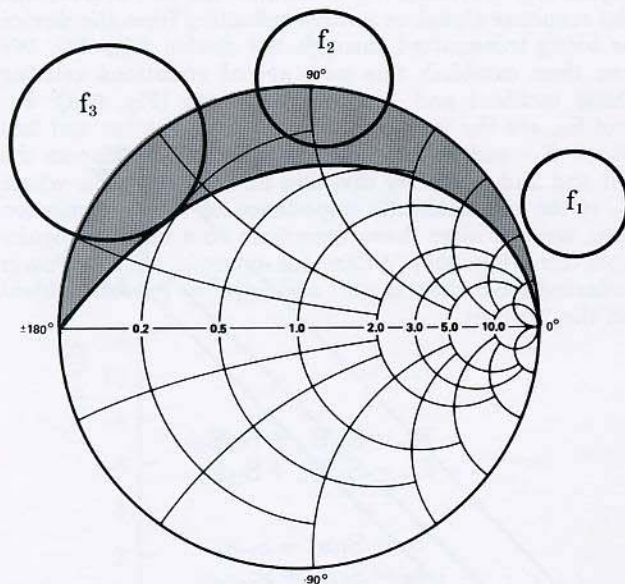


Figure 64

Stability is strongly dependent on the  $|S_{12}| |S_{21}|$  product (Fig. 65).  $|S_{21}|$  is a generally decreasing function of frequency from  $f_\beta$  on.

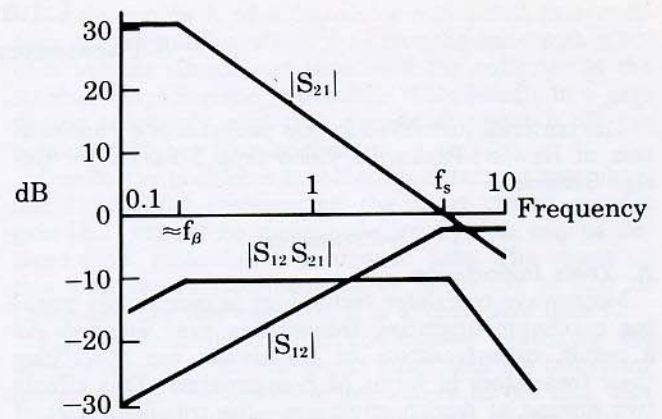


Figure 65

$|S_{12}|$  is an increasing function.

Looking at the  $|S_{12}| |S_{21}|$  product, we see that it increases below  $f_\beta$ , flattens out, then decreases at higher frequencies.

It is in this flat region that we must worry about instability.

On the other hand, if we synthesize elements such as inductors by using high impedance transmission lines, we might have capacitance rather than inductance at higher frequencies, as seen here on the Impedance Phase plot (Fig. 66). If we suspect that this might cause oscillation, we would investigate stability in the region where the inductor is capacitive. Using tunnel diodes having negative impedance all the way down to dc, we would have to investigate stability right on down in frequency to make sure that oscillations did not occur outside the band in which we are working.

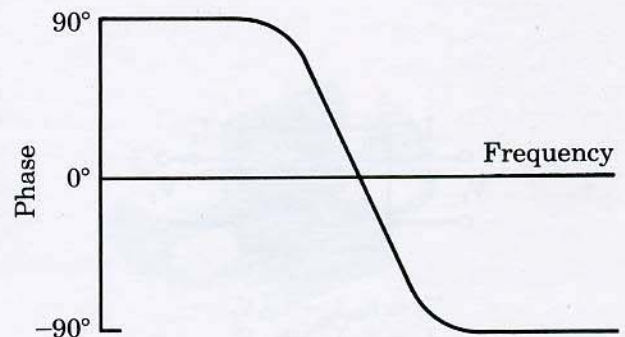


Figure 66

# Chapter III

## S-Parameter Measurements

The material presented in this program is a continuation of Hewlett-Packard's video tape S-Parameter Design Seminar.

### S-Parameters

#### A. Their Importance

Microwave transistor technology is continually pushing maximum operating frequencies ever upward. As a result, manufacturers of transistors are specifying their transistors in terms of S-parameters. This affects two groups of design engineers—the transistor circuit designer must now switch his thinking from the well-known H, Y, and Z-parameters in his circuit design to the S or scattering parameters.

The microwave engineer, since transistor technology is moving into his frequency domain, must now become conversant with transistor terminology and begin to think of applying transistors to the circuits he works with.

In this tape we will:

1. Review the S-parameter concept.
2. Show the results of typical S-parameter measurements of a 12 GHz transistor.
3. Demonstrate the network analyzer system used in these measurements.

#### B. Review of S-Parameters

The function of network analysis is to completely characterize or describe a network so we'll know how it will behave when stimulated by some signal. For a two-port device, such as transistors, we can completely describe or characterize it by establishing a set of equations that relate the voltages and currents at the two ports (Fig. 67).

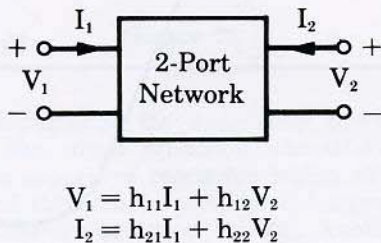


Figure 67

In low frequency transistor work, one such set of equations relates total voltages across the ports and total current into or out of these ports in terms of H-parameters. For example,

$$h_{11} = \frac{V_1}{I_1} \Big|_{V_2 = 0}$$

These parameters are obtained under either open or short circuit conditions.

At higher frequencies, especially in the microwave domain, these operating conditions present a problem since a short circuit looks like an inductor and an open circuit has some leakage capacitance. Often, if the network is an active device such as a transistor, it will oscillate when terminated with a reactive load.

It is imperative that some new method for characterizing these devices at high frequencies has to be used.

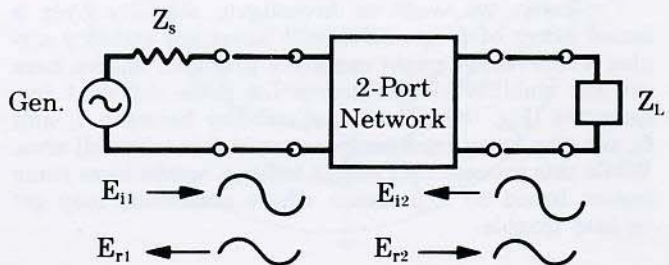


Figure 68

If we embed our two-port device into a transmission line, and terminate the transmission line in its characteristic impedance, we can think of the stimulus signal as a traveling wave incident on the device, and the response signal as a wave reflecting from the device or being transmitted through the device (Fig. 68). We can then establish this new set of equations relating these incident and "scattered" waves (Fig. 69a):  $E_{1r}$  and  $E_{2r}$  are the voltages reflected from the 1st and 2nd ports,  $E_{1i}$  and  $E_{2i}$  are the voltages incident upon the 1st and 2nd ports. By dividing through by  $\sqrt{Z_0}$ , where  $Z_0$  is the characteristic impedance of the transmission line, we can alter these equations to a more recognizable form (Fig. 69b). Where, for example,  $|b_1|^2 = \text{Power reflected from the 1st port}$  and  $|a_1|^2 = \text{Power incident on the 1st port}$ .

$$\begin{aligned} \text{a) } E_{1r} &= S_{11}E_{1i} + S_{12}E_{2i} \\ E_{2r} &= S_{21}E_{1i} + S_{22}E_{2i} \\ \text{b) } b_1 &= S_{11}a_1 + S_{12}a_2 \\ b_2 &= S_{21}a_1 + S_{22}a_2 \end{aligned}$$

$$\text{where } b_N = \frac{E_{Nr}}{\sqrt{Z_0}} \quad \text{and} \quad a_N = \frac{E_{Ni}}{\sqrt{Z_0}}$$

Figure 69

$S_{11}$  is then equal to  $b_1/a_1$  with  $a_2 = 0$  or no incident wave on port 2. This is accomplished by terminating the output of the two-port in an impedance equal to  $Z_0$ .

### C. Summary

$S_{11}$  = input reflection coefficient with the output matched.

$S_{21}$  = forward transmission coefficient with the output matched.

This is the gain or attenuation of the network.

$S_{22}$  = output reflection coefficient with the input matched.

$S_{12}$  = reverse transmission coefficient with the input matched.

To the question "Why are S-parameters important?" you can now give several answers:

1. S-parameters are determined with resistive terminations. This obviates the difficulties involved in obtaining the broadband open and short circuit conditions required for the H, Y, and Z-parameters.
2. Parasitic oscillations in active devices are minimized when these devices are terminated in resistive loads.
3. Equipment is available for determining S-parameters since only incident and reflected voltages need to be measured.

### Characterization of Microwave Transistors

Now that we've briefly reviewed S-parameter theory, let's look at some typical transistor parameters. There are three terms often used by transistor circuit designers (Fig. 70):

1.  $f_t$  or the frequency at which the short circuit current gain is equal to one;
2.  $f_s$  or the frequency where  $|S_{21}| = 1$  or the power gain of the device,  $|S_{21}|^2$ , expressed in dB is zero;
3.  $f_{max}$  or the frequency where the maximum available power gain,  $G_{AMAX}$ , of the device is equal to one.  $f_{max}$  is also referred to as the maximum frequency of oscillation.

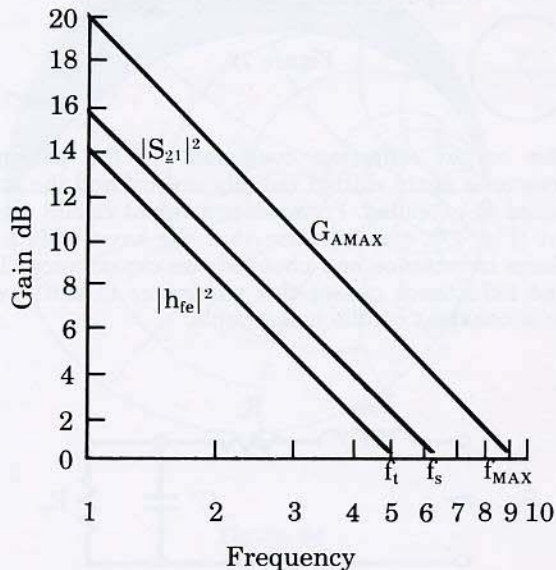


Figure 70

To determine  $f_s$  of a transistor connected in a common emitter configuration, we drive the base with a 50-ohm voltage source and terminate the collector in the 50-ohm characteristic impedance. This results in a gain versus frequency plot that decays at about 6 dB per octave at higher frequencies.

Due to the problems involved in obtaining true short circuits at high frequencies, the short circuit current gain  $|h_{fe}|$  cannot be measured directly, but can be derived from measured S-parameter data. The shape of this gain versus frequency curve is similar to that of  $|S_{21}|^2$  and, for this example,  $f_t$  is slightly less than  $f_s$ .

$f_{max}$  is determined after conjugately matching the voltage source to the transistor input, and the transistor output to the characteristic impedance of the line. The resulting gain is the maximum available power gain as a function of frequency. It is higher than  $|S_{21}|^2$  because of impedance matching at the input and output. With proper impedance matching techniques, the transistor is usable above  $f_s$  in actual circuit design.

### S-Parameters of Transistors

#### A. Introduction

Let's now shift our attention to the actual S-parameters of a transistor. We'll look at transistors in chip form and after the chips have been packaged. The advantage of characterizing the chip is that you will get a better qualitative understanding of the transistor. However, fixtures to hold these chips are not readily available. Most engineers will be using packaged transistors in their R&D work. There are fixtures available for characterizing packaged transistors, and we will demonstrate these later on (Fig. 71). The bias conditions used when obtaining these transistors' parameters connected as common emitter:  $V_{cb} = 15$  V and  $I_c = 15$  mA.

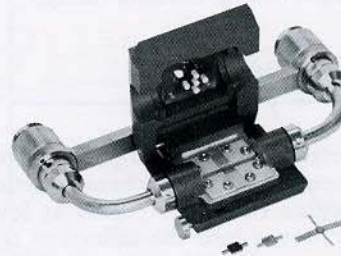


Figure 71

#### B. $S_{11}$ of Common Emitter

The input reflection characteristic,  $S_{11}$ , of the chip transistor seems to be following a constant resistance circle on the Smith Chart (Fig. 72). At lower frequencies, the capacitive reactance is clearly visible and, as the frequency increases, this reactance decreases and the resistance becomes more evident. A small inductance is also evident which, for this example, resonates with the capacitance at 10 GHz.

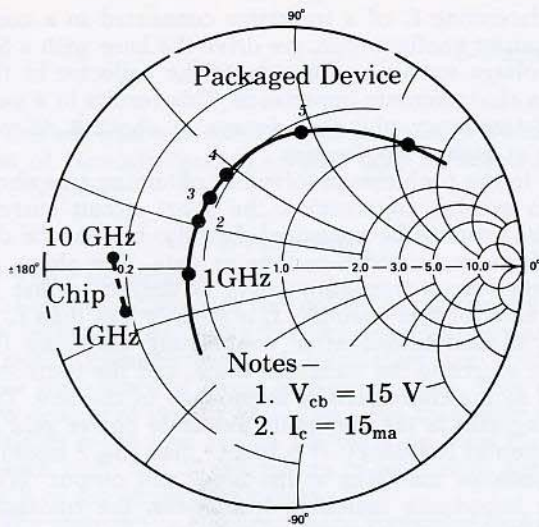


Figure 72

An equivalent circuit can be drawn that exhibits such characteristics (Fig. 73). The resistance comes from the bulk resistivities in the transistor's base region plus any contact resistance resulting from making connections to the device. The capacitance is due mainly to the base-emitter junction. The inductance results from the emitter resistance being referred back to the input by a complex  $\beta$  at these high frequencies.

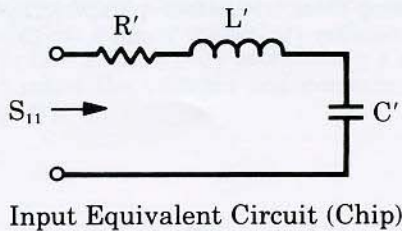


Figure 73

If you characterize the same chip transistor after packaging, the input reflection characteristic again starts in the capacitive reactance region at lower frequencies and then moves into the inductive reactance region at higher frequencies (Fig. 72). Another equivalent circuit explaining this characteristic can be drawn (Fig. 74). Package inductance and capacitance contribute to the radial shift inward as well as to the extension of the  $S_{11}$  characteristic into the upper portion of the Smith Chart.

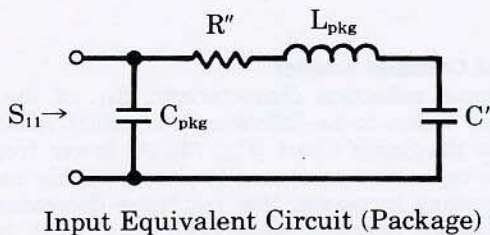


Figure 74

### C. $S_{22}$ of Common Emitter

The output reflection coefficient,  $S_{22}$ , is again in the capacitive reactance portion of the Smith Chart (Fig. 75). If you overlay an admittance Smith Chart, you can see that this characteristic roughly follows a constant conductance circle. This type of characteristic represents a shunt RC type of equivalent circuit where the angle spanned would be controlled by capacitive elements, and the radial distance from the center of the Smith Chart would be a function of the real parts (Fig. 76).

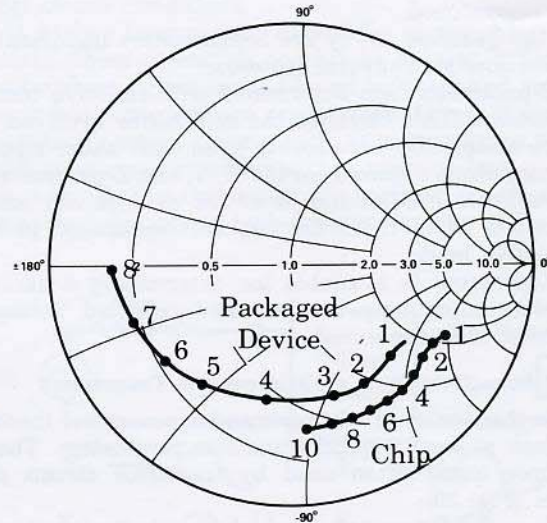
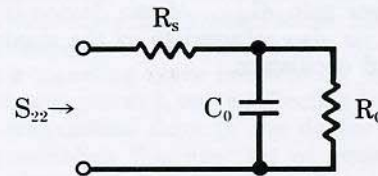


Figure 75



Output Equivalent Circuit (Chip)

Figure 76

The output reflection coefficient of the packaged transistor is again shifted radially inward and the angle spanned is extended. From an equivalent circuit standpoint (Fig. 77), you can see that we have added the package inductance and changed the capacitance. This added inductance causes this parameter to shift away from a constant conductance circle.

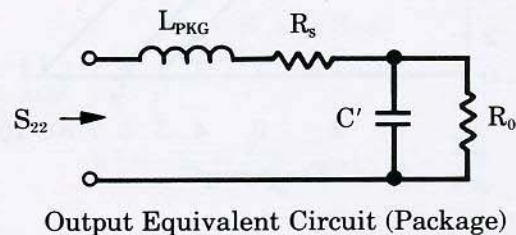


Figure 77

### D. $S_{21}$ of Common Emitter

The forward transmission coefficient,  $S_{21}$ , that we have seen before when discussing  $f_s$ , exhibits a voltage gain value slightly greater than 4 or 12 dB at 1 GHz and crosses the unity gain circle between 4 and 5 GHz (Fig. 78). The packaged transistor exhibits slightly less gain and a unity gain crossover at around 4 GHz.

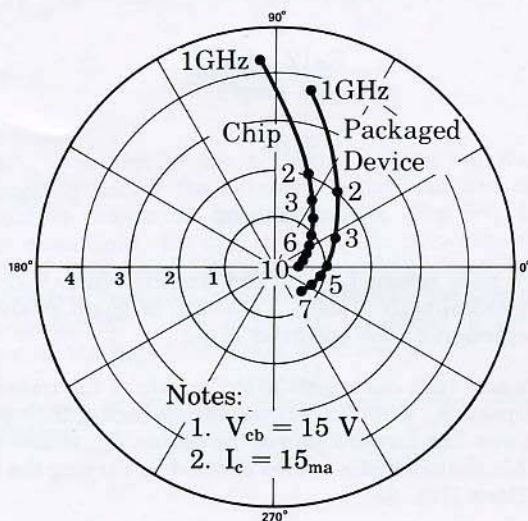


Figure 78

In an equivalent circuit, we could add a current source as the element giving gain to the transistor (Fig. 79).

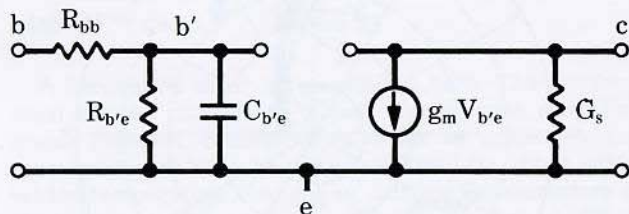


Figure 79

### E. $S_{12}$ of Common Emitter

Since a transistor is not a unilateral device, the reverse transmission characteristic,  $S_{12}$ , will have some finite value in chip form. On a polar plot, the  $S_{12}$  characteristic approximates a circular path (Fig. 80).

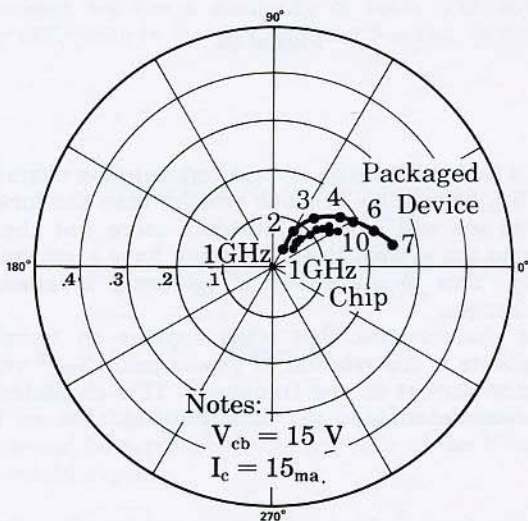


Figure 80

If you were to plot  $|S_{12}|$  on a Bode Diagram, you would see a gradual buildup at about 6 dB/octave at low frequencies, a leveling off and then ultimately a decay at the higher frequencies. Let's now superimpose a Bode Plot of  $|S_{21}|$ . It is constant at frequencies below  $f_\beta$  and then decays at about 6 dB/octave. Therefore, the product of these two characteristics would increase up to  $f_\beta$ , around 100 to 200 MHz, and remain relatively flat until a break point at around the  $f_s$  of the transistor (Fig. 81).

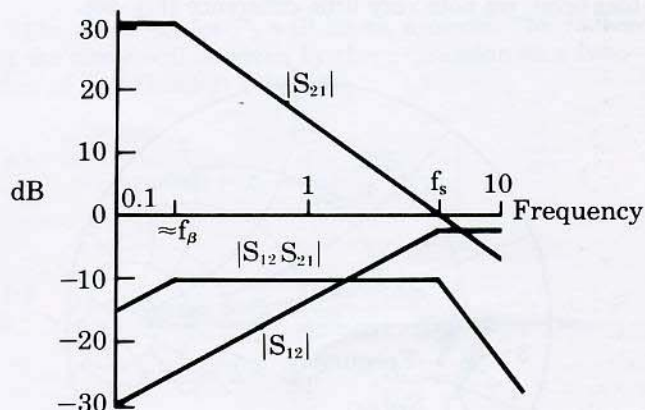


Figure 81

This  $|S_{12}| |S_{21}|$  product is significant since it both represents a figure of merit of the feedback or stability term of the device and it also appears in the complete equations for input and output reflection coefficients.

### F. Combined Equivalent Circuit

If you were to now combine the equivalent circuits drawn up to this point, you could arrive at a **qualitative** model that describes the transistor's operation (Fig. 82).

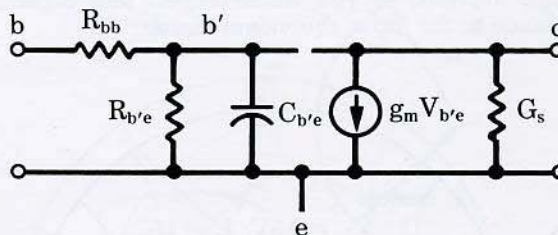


Figure 82

### Measurement Demonstration

Now that you've seen some typical transistor characteristics, let's actually make several measurements to see how simply and accurately you can make the measurements that will provide you with the necessary data for designing your circuits.

The S-parameter characteristics we have seen are those of a Model 35821E Transistor. In these measurements we will measure the transistor in a K-disc common emitter package.

The standard bias conditions are:  $V_{cb} = 15$  volts  
 $I_c = 15$  mA

On the polar display with the Smith Chart overlay inserted, the input impedance can be read off directly. To ensure that we are in the linear region of the transistor, we can measure  $S_{11}$  at two input power levels to the transistor. If these readings do not change, we know that we are driving the transistor at an optimum power level and the S-parameters are truly the small signal characteristics. If we now vary the collector current bias level, we note very little difference (Fig. 90).

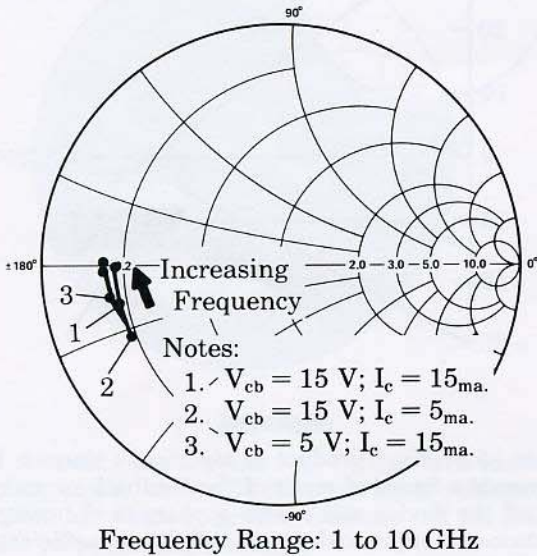


Figure 90

Returning the current level to the original value, we now decrease  $V_{cb}$  and note a shift of the original characteristic. Decreasing  $V_{cb}$  causes the epitaxial layer to be less depleted so you would expect less capacitive reactance in the input equivalent circuit.

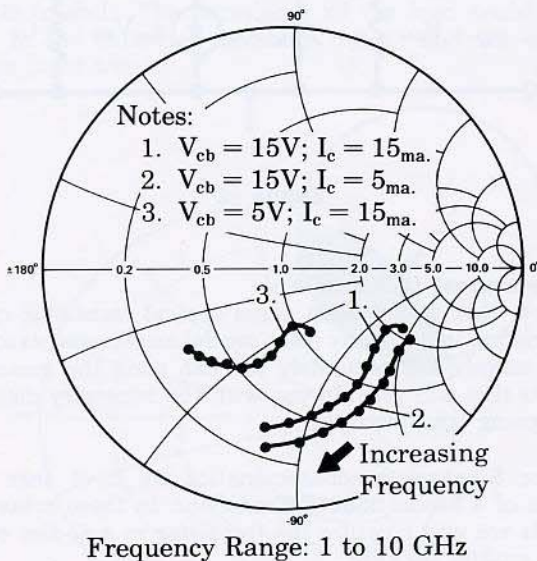


Figure 91

Now you can measure the output reflection coefficient (Fig. 91). Let's now reduce the collector current and note the effect on this characteristic. The radial shift outward indicates an increase in the real part of the output impedance. This shift is due to the real part being inversely proportional to the  $g_m$  of the transistor, while the collector current is directly proportional to  $g_m$  (Fig. 92).

$$\text{Re}[Z_{out}] \propto \frac{1}{g_m}$$

$$I_c \propto g_m$$

Figure 92

Let's now return  $I_c$  to 15 mA and decrease  $V_{cb}$ . You note a radial shift inward. This shift is again related to the depletion of the epitaxial layer.

Let's now turn our attention to the gain of the transistor and depress  $S_{21}$  with the bias conditions back at their original values. The forward gain of the device,  $S_{21}$ , is now visible. This characteristic is also affected by varying the bias conditions (Fig. 93).

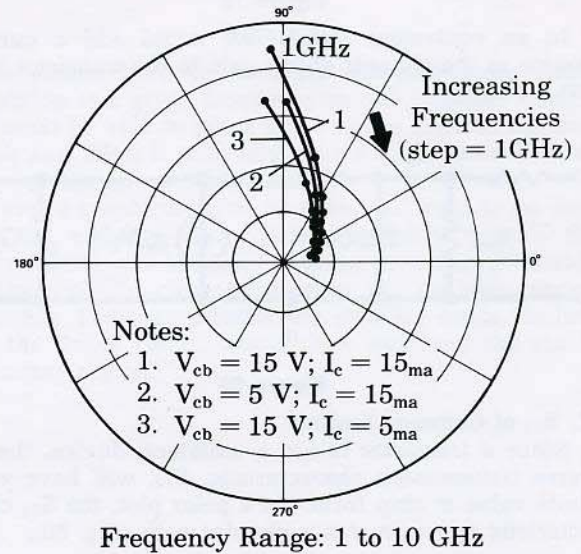


Figure 93

Let's look now at the reverse transmission characteristic,  $S_{12}$ . This value is much smaller than the forward gain, so we will have to introduce more test channel gain into the system to enable us to have a reasonable display. This characteristic is relatively invariant to bias changes.

One characteristic that often appears on transistor data sheets is the relation of power gain  $|S_{21}|^2$  versus collector current at one frequency. This characteristic curve was determined at 1 GHz (Fig. 94).

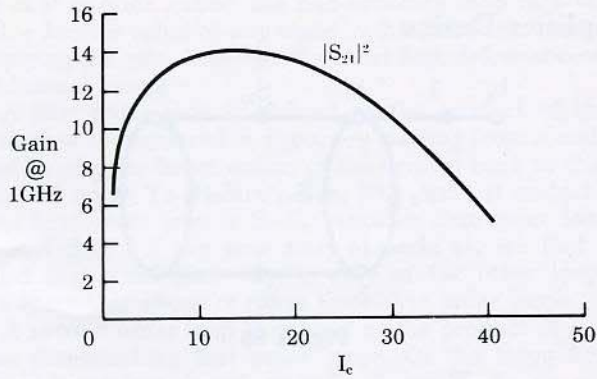


Figure 94

At low current levels, there is a gradual increase, then the power gain characteristic flattens out and decreases at higher current levels. The base-collector transit time determines the flat plateau. The high current roll-off is due to two effects: (1) thermal effects on the transistor; (2) if we try to pump more current into the device than it can handle, the base of the transistor stretches electrically. Since the electrons move across the base-collector junction at a finite rate, the current density increases as we try to pump more current in, until, at the limit, the base has stretched to the width of the epitaxial layer and this will account for the gain going toward zero.

### Summary

This tape has presented an overview of S-parameter theory and has related this theory to actual transistor characterization.

The remaining tapes in this S-Parameter Design Seminar are devoted to high frequency circuit design techniques using S-parameters. Constant gain and noise figure circles will be discussed and then used in designing unilateral narrow and broadband amplifiers.

This amplifier (Fig. 95), for example, was designed with S-parameter data, and operates from 100 MHz to 2 GHz with a typical gain of 40 dB and flat to within 3 dB across the band. A similar amplifier will be designed in the next tape.



Figure 95

The use of these design techniques and measurement equipment will also prove valuable to you in your device development.

# Chapter IV

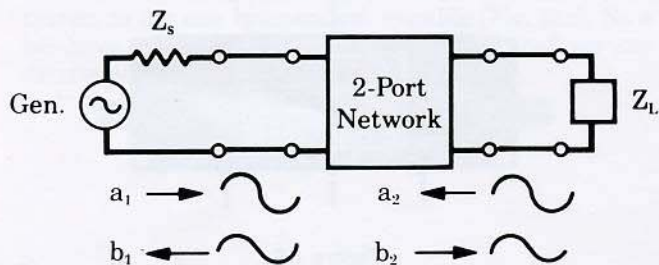
## High Frequency Amplifier Design

### Introduction

In this tape, the practical application of S-parameters will be discussed. They will specifically be applied to unilateral amplifier design. This tape is a continuation of the Hewlett-Packard Microwave Division's S-Parameter Design Seminar. We will discuss: Transducer Power Gain, Constant Gain and Constant Noise Figure Circles, and then use these concepts with S-parameter data in the design of amplifiers for the case where the transistor can be assumed to be unilateral, or  $S_{12} = 0$ .

### S-Parameter Review

Before introducing these concepts, let's briefly review S-parameters.



If:  $Z_L = Z_0, \quad a_2 = 0$

Figure 96

As opposed to the more conventional parameter sets which relate total voltages and total currents at the network ports, S-parameters relate **traveling waves** (Fig. 96). The **incident** waves,  $a_1$  and  $a_2$ , are the independent variables and the **reflected** waves,  $b_1$  and  $b_2$ , are the dependent variables. The network is assumed to be embedded in a transmission line system of known characteristic impedance which shall be designated  $Z_0$ . The S-parameters are then measured with  $Z_0$  terminations on each of the ports of the network. Under these conditions,  $S_{11}$  and  $S_{22}$ , the input and output reflection coefficients, and  $S_{21}$  and  $S_{12}$ , the forward and reverse transmission coefficients, can be measured (Fig. 97).

$$S_{11} = \left. \frac{b_1}{a_1} \right|_{a_2 = 0} \quad S_{12} = \left. \frac{b_1}{a_2} \right|_{a_1 = 0}$$

$$S_{21} = \left. \frac{b_2}{a_1} \right|_{a_2 = 0} \quad S_{22} = \left. \frac{b_2}{a_2} \right|_{a_1 = 0}$$

Figure 97

### Transducer Power Gain

In the design of amplifiers, we are most interested in the transducer power gain. An expression can be derived for transducer power gain if we first redraw the two-port network using flow graph techniques (Fig. 98).

The transducer power gain is defined as the power delivered to the load divided by the power available from the source. The ratio of  $b_2$  to  $b_s$  can be found by applying the non-touching loop rule for flow graphs resulting in this expression for transducer power gain (Fig. 99).

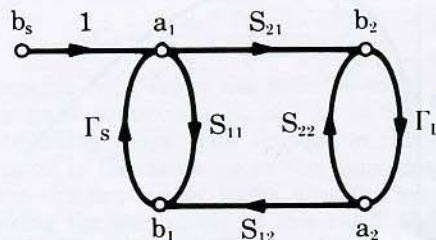


Figure 98

$$G_T = \frac{P_{del}}{P_{avs}}$$

$$= \frac{|b_2|^2(1 - |\Gamma_L|^2)}{|b_s|^2(1 - |\Gamma_s|^2)}$$

$$= \frac{|S_{21}|^2(1 - |\Gamma_s|^2)(1 - |\Gamma_L|^2)}{|(1 - S_{11}\Gamma_s)(1 - S_{22}\Gamma_L) - S_{21}S_{12}\Gamma_L\Gamma_s|^2}$$

Figure 99

If we now assume the network to be unilateral, that is,  $S_{12}$  is equal to zero, this term ( $S_{21}S_{12}\Gamma_L\Gamma_s$ ) drops out and the resulting expression can be separated into three distinct parts. This expression will be referred to as the **unilateral** transducer power gain (Fig. 100).

$$G_{Tu} = |S_{21}|^2 \cdot \frac{(1 - |\Gamma_s|^2)}{|1 - S_{11}\Gamma_s|^2} \cdot \frac{(1 - |\Gamma_L|^2)}{|1 - S_{22}\Gamma_L|^2}$$

Figure 100

The first term is related to the transistor or other active device being used. Once the device and its bias conditions are established,  $S_{21}$  is determined and remains invariant throughout the design.

The other two terms, however, are not only related to the remaining S-parameters of the two-port device,  $S_{11}$  and  $S_{22}$ , but also to the source and load reflection coefficients. It is these latter two quantities which we will be able to control in the design of the amplifier. We will employ lossless impedance transforming networks at the input and output ports of the network. We can then think of the unilateral transducer power gain as being made up of three distinct and independent gain terms and the amplifier as three distinct gain blocks (Fig. 101).

$$G_{Tu} = \frac{(1 - |\Gamma_s|^2)}{|1 - S_{11}\Gamma_s|^2} \cdot |S_{21}|^2 \cdot \frac{(1 - |\Gamma_L|^2)}{|1 - S_{22}\Gamma_L|^2}$$

$$= G_s \cdot G_0 \cdot G_L$$

$$= G_{sDB} + G_{0DB} + G_{LDB}$$

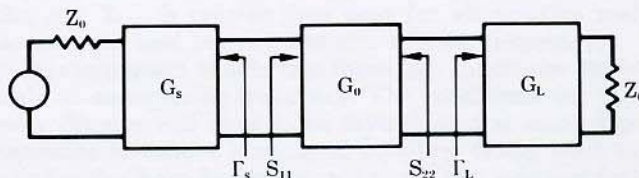


Figure 101



The  $G_s$  term affects the degree of mismatch between the characteristic impedance of the source and the input reflection coefficient of the two-port device. Even though the  $G_s$  block is made up of passive components, it can have a gain contribution greater than unity. This is true because an intrinsic mismatch loss exists between  $Z_o$  and  $S_{11}$  and the impedance transforming elements can be employed to improve this match, thus decreasing the mismatch loss, and can, therefore, be thought of as providing gain.

The  $G_o$  term is, as we said before, related to the device and its bias conditions and is simply equal to  $|S_{21}|^2$ .

The third term in the expression,  $G_L$ , serves the same function as the  $G_s$  term, but affects the matching at the output rather than the input.

Maximum unilateral transducer gain can be accomplished by choosing impedance matching networks such that  $\Gamma_s = S_{11}^*$  and  $\Gamma_L = S_{22}^*$  (Fig. 102).

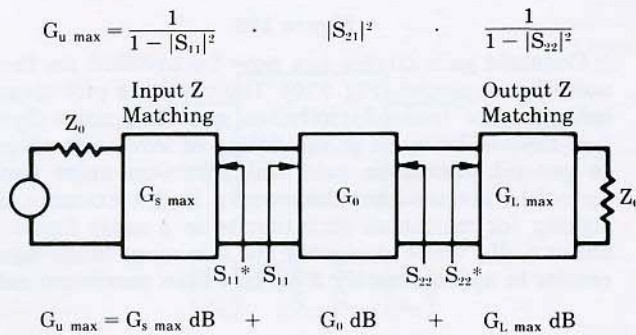


Figure 102

### Constant Gain Circles

Let's look at the  $G_s$  term now in a little more detail. We have just seen that for  $\Gamma_s = S_{11}^*$ ,  $G_s$  is equal to a maximum. It is also clear that for  $|\Gamma_s| = 1$ ,  $G_s$  has a value of zero. For any arbitrary value of  $G_s$  between these extremes of zero and  $G_s$  max, solutions for  $\Gamma_s$  lie on a circle (Fig. 103).

For  $G_s = 0 < g < G_{s \max}$

$$g = \frac{1 - |\Gamma_s|^2}{|1 - \Gamma_s S_{11}|^2}$$

Figure 103

It is convenient to plot these circles on a Smith Chart. The circles have their centers located on the vector drawn from the center of the Smith Chart to the point  $S_{11}^*$  (Fig. 104).

These circles are interpreted as follows:

Any  $\Gamma_s$  along a 2 dB circle would result in a  $G_s = 2$  dB.

Any  $\Gamma_s$  along the 0 dB circle would result in a  $G_s = 0$  dB, and so on.

For points in this region (within the 0 dB circle), the impedance transforming network is such as to improve the input impedance match and for points in this region (area outside the 0 dB circle), the device is further mismatched. These circles are called **constant gain circles**.

Since the expression for the output gain term,  $G_L$ , has the same form as that of  $G_s$ , a similar set of constant gain circles can be drawn for this term. These circles can be located precisely on the Smith Chart by applying these formulas (Fig. 105):

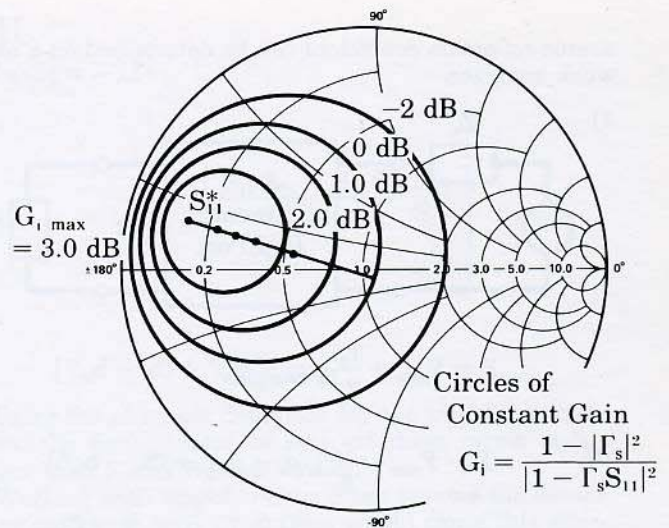


Figure 104

$$d_i = \frac{g_i |S_{11}|}{1 - |S_{11}|^2 (1 - g_i)}$$

$$R_i = \frac{\sqrt{1 - g_i} (1 - |S_{11}|^2)}{1 - |S_{11}|^2 (1 - g_i)}$$

$$g_i = G_i (1 - |S_{11}|^2) = \frac{G_i}{G_{i \max}}$$

$G_i$  = Gain represented by the circle.

Figure 105

1.  $d_i$  being the distance from the center of the Smith Chart to the center of the constant gain circle along the vector  $S_{11}^*$
2.  $R_i$  is the radius of the circle and
3.  $g_i$  is the normalized gain value for the gain circle  $G_i$ .

### Constant Noise-Figure Circuits

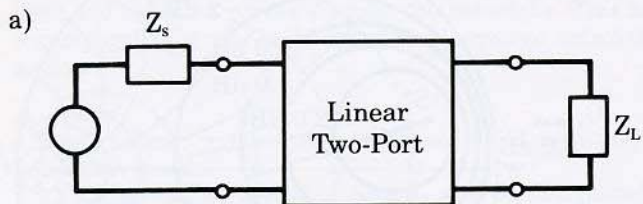
Another important aspect of amplifier design is noise figure, which is defined as the ratio of the S/N ratio at the input to the S/N ratio at the output.  $NF = \frac{S/N \text{ in}}{S/N \text{ out}}$

In general, the noise figure for a linear two-port has this form (Fig. 106a), where  $r_n$  is the equivalent input noise resistance of the two-port.  $G_s$  and  $b_s$  represent the real and imaginary parts of the source admittance, and  $g_o$  and  $b_o$  represent the real and imaginary parts of that source admittance which results in the minimum noise figure,  $F_{\min}$ .

If we now express  $Y_s$  and  $Y_o$  in terms of reflection coefficients and substitute these equations in the noise figure expression, we see once again that the resulting equation has the form of a circle (Fig. 106B). For a given noise figure,  $F$ , the solutions for  $\Gamma_s$  will lie on a circle. The equations for these circles can be found given the parameters  $\Gamma_o$ ,  $F_{\min}$ , and  $r_n$ . Unless accurately specified on the data sheet for the device being used, these quantities must be found experimentally.

Generally, the source reflection coefficient would be varied by means of a slide screw tuner or stub tuners to obtain a minimum noise figure as read on a noise figure meter.  $F_{\min}$  can then be read off the meter and the

source reflection coefficient can be determined on a network analyzer.



$$F = F_{\min} + \frac{r_n}{g_s} [(g_s - g_0)^2 + (b_s - b_0)^2]$$

b)

$$F - F_{\min} = \frac{r_n}{g_s} [(g_s - g_0)^2 + (b_s - b_0)^2]$$

Substitute  $Y_s = \frac{1 - \Gamma_s}{1 + \Gamma_s}$ ,  $Y_0 = \frac{1 - \Gamma_0}{1 + \Gamma_0}$

$$F - F_{\min} = 4r_n \frac{|\Gamma_s - \Gamma_0|^2}{(1 - |\Gamma_s|^2)|1 + \Gamma_0|^2}$$

To Find  $r_n$ , Measure  $F$  for  $\Gamma_s = 0$

$$4r_n = [F_{\Gamma_s=0} - F_{\min}] \frac{|1 + \Gamma_0|^2}{|\Gamma_0|^2}$$

**Figure 106**

The equivalent noise resistance,  $r_n$ , can be found by making one additional noise figure reading with a known source reflection coefficient. If a 50-ohm source were used, for example,  $\Gamma_s = 0$  and this expression could be used to calculate  $r_n$  (Fig. 107).

For  $\Gamma_s = 0$

$$r_n = [F_{\Gamma_s=0} - F_{\min}] \frac{|1 + \Gamma_0|^2}{4|\Gamma_0|^2}$$

**Figure 107**

To determine a family of noise figure circles, let's first define a noise figure parameter,  $N_i$ :

$$N_i = \frac{F_i - F_{\min}}{4r_n} \cdot |1 + \Gamma_0|^2$$

Here,  $F_i$  is the value of the desired noise figure circle and  $\Gamma_0$ ,  $F_{\min}$ , and  $r_n$  are as previously defined. With a value for  $N_i$  determined, the center and radius of the circle can be found by these expressions (Fig. 108).

$$C_{F_i} = \frac{\Gamma_0}{1 + N_i}$$

$$R_{F_i} = \frac{1}{1 + N_i} \sqrt{N_i^2 + N_i(1 - |\Gamma_0|^2)}$$

**Figure 108**

From these equations, we see that  $N_i = 0$  where  $F_i = F_{\min}$ , and the center of the  $F_{\min}$  circle with zero radius is located at  $\Gamma_0$  on the Smith Chart. The centers of the other noise figure circles lie along the  $\Gamma_0$  vector.

This plot then gives the noise figure for a particular device for any arbitrary source impedance at a particular frequency (Fig. 109). For example, given a source impedance of  $40 + j 50$  ohms, the noise figure would be 5 dB. Likewise, a source of 50 ohms would result in a noise figure of approximately 3.5 dB.

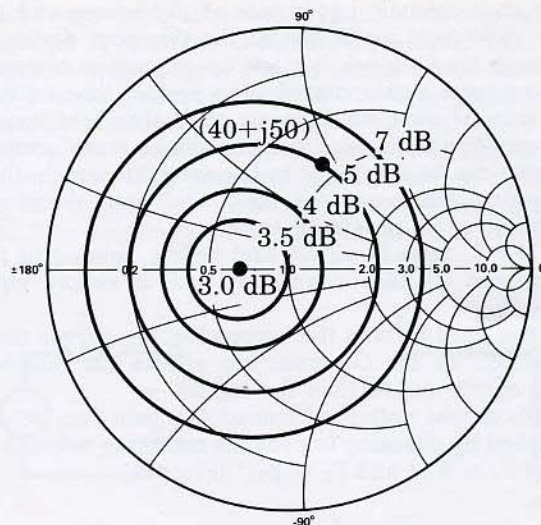


**Figure 109**

Constant gain circles can now be overlaid on these noise figure circles (Fig. 110). The resulting plot clearly indicates the tradeoffs between gain and noise figure that have to be made in the design of low noise stages. In general, maximum gain and minimum noise figure cannot be obtained simultaneously. In this example, designing for maximum gain results in a noise figure of about 6 dB, while designing for minimum noise figure results in approximately 2 dB less than maximum gain.

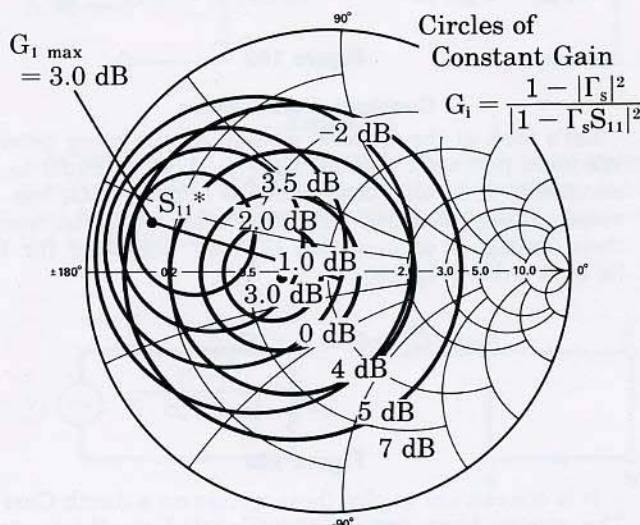


**Figure 110**

The relative importance of the two design objectives, gain and noise figure, will dictate the compromise that must be made in the design.

It is also important to remember that the contributions of the second stage to the overall amplifier noise figure can be significant, especially if the first stage gain is low (Fig. 111). It is, therefore, not always wise to minimize first stage noise figure if the cost in gain is

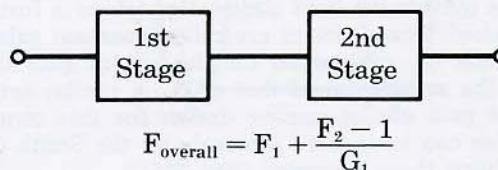


**Figure 111**

too great. Very often there is a better compromise between first stage gain and noise figure which results in a lower overall amplifier noise figure.

### Design Examples

With the concepts of constant gain and constant noise figure circles well in hand, let's now embark on some actual design examples.

Shown here is a typical single stage amplifier with the device enmeshed between the input and output matching networks (Fig. 112). The device we will be using for the design examples is a HP-21, 12 GHz transistor.

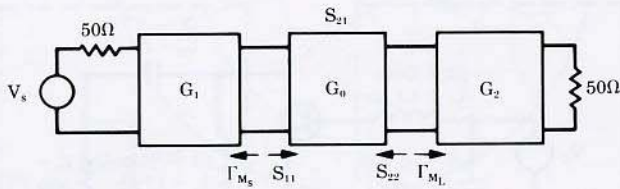
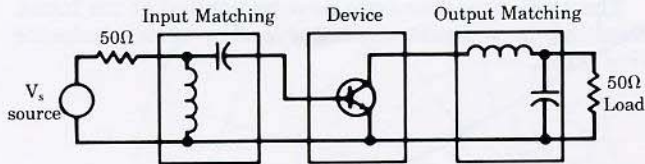


Figure 112

The forward gain characteristic,  $S_{21}$ , of this particular transistor was measured in the previous video tape of this seminar, and we noted that  $|S_{21}|^2$  is a decreasing function with frequency having a slope of approximately 6 dB per octave.  $G_{u\max}$ , which is the maximum unilateral transducer gain, is essentially parallel to the forward gain curve (Fig. 113). This is not necessarily true in general, but in this case, as we can see on this Smith Chart plot, the magnitudes of  $S_{11}$  and  $S_{22}$  for this device are essentially constant over the frequency band in question (Fig. 114). Thus, the maximum values of the input and output matching terms are also relatively constant over this frequency range.

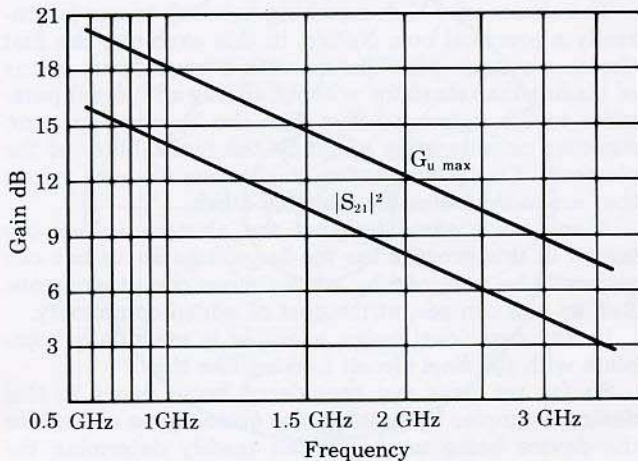


Figure 113

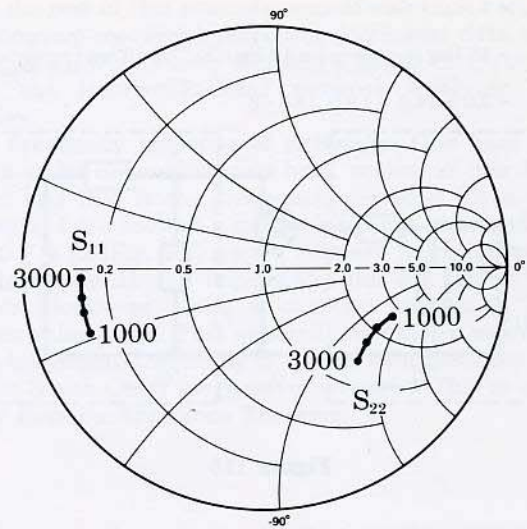


Figure 114

To illustrate the various considerations in the design of unilateral amplifier stages, let's select three design examples (Fig. 115). In the first example, we want to design an amplifier stage at 1 GHz having a gain equal to  $G_{u\max}$ , which in this case is 18.3 dB. No consideration will be given in this design to noise figure. In the second example, we will aim for minimum noise figure with a gain of 16 dB. The third example will be the design of an amplifier covering the frequency band from 1 to 2 GHz with a minimum gain of 10 dB and a noise figure less than 4.5 dB.

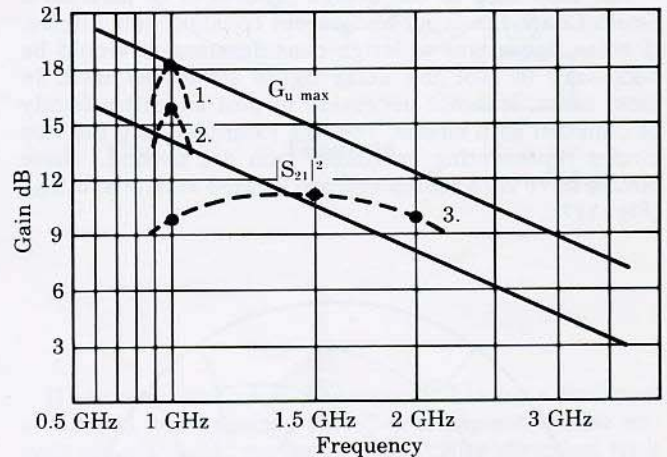


Figure 115

In these examples, we will assume a source impedance and a load impedance of 50 ohms. In general, however, the source impedance could be complex such as the output impedance of the previous stage. Likewise, the output load is quite often the input impedance of a following stage.

#### A. Design for $G_{u\max}$

Now in this first example since we will be designing for  $G_{u\max}$  at 1 GHz, the input matching network will be designed to conjugate match the input impedance of the transistor. This will provide a net gain contribution of 3 dB (Fig. 116).

$$\begin{aligned}
 G_{u \max} &= G_{1 \max} + G_0 + G_{2 \max} \\
 &= 10 \text{ Log} \left( \frac{1}{1 - |S_{11}|^2} \right) + 10 \text{ log} (|S_{21}|^2) + 10 \text{ log} \left( \frac{1}{1 - |S_{22}|^2} \right) \\
 &= 3.0 + 14.0 + 1.3 = 18.3 \text{ dB}
 \end{aligned}$$

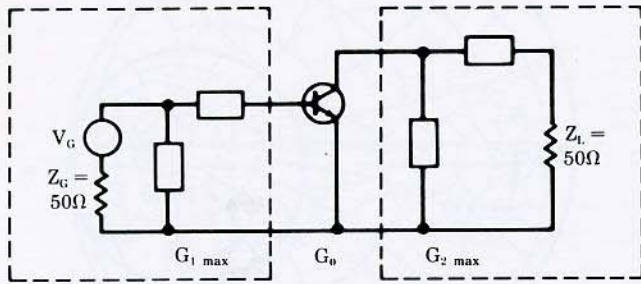


Figure 116

The output matching network will be used to conjugately match the 50-ohm load impedance to the output impedance of the transistor. From the measured data for  $S_{22}$  at 1 GHz, we find that this matching network will provide a gain contribution of 1.3 dB at the output.

Since the gain of the transistor at 1 GHz with 50-ohm source and load termination is 14 dB, the overall gain of this single stage amplifier will be 18.3 dB. The matching elements used can be any routine element—this includes inductors, capacitors, and transmission lines.

In general, to transform one impedance to any other impedance at one frequency requires two variable elements. A transmission line does, by itself, comprise two variables in that both its impedance and its length can be varied. In our example, however, we will use only inductors and capacitors for the matching elements.

The next step in the design process is to plot, on a Smith Chart, the input and output constant gain circles. If noise figure was a design consideration, it would be necessary to plot the noise figure circles as well. In most cases, it is not necessary to plot an entire family of constant gain circles. For this example, only the two circles representing maximum gain are needed. These circles have zero radius and are located at  $S_{11}^*$  and  $S_{22}^*$  (Fig. 117).

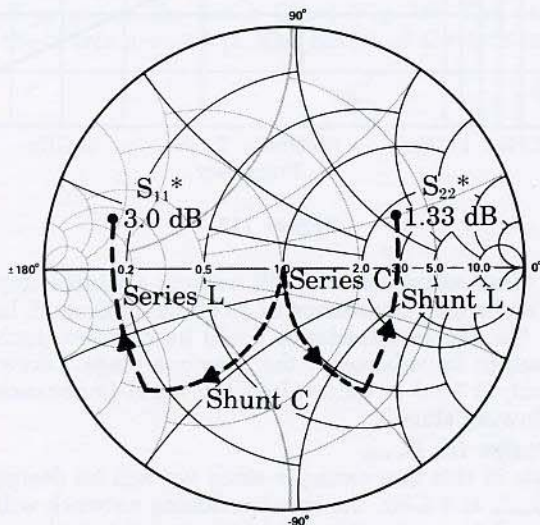


Figure 117

To facilitate the design of the matching networks, let's first overlay another Smith Chart on the one we now have. This added Smith Chart is oriented at  $180^\circ$  angle with respect to the original chart. The original chart can then be used to read impedances and the overlaid chart to read admittances.

To determine the matching network for the output, we start from our load impedance of 50 ohms at the center of the chart and proceed along a constant resistance circle until we arrive at the constant conductance circle which intersects the point representing  $S_{22}^*$ . This represents a negative reactance of 75 ohms. Hence, the first element is a series capacitor.

We now add an inductive susceptance along the constant conductance circle so that the impedance looking into the matching network will be equal to  $S_{22}^*$ .

The same procedure can now be applied at the input, resulting in a shunt capacitor and a series inductor (Fig. 118).

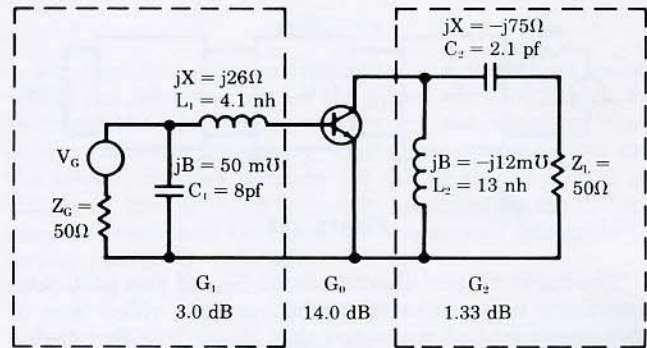


Figure 118

There are, of course, other networks which would accomplish the purpose of matching the device to the 50-ohm load and source. We could, for example, have added an inductive reactance and then a shunt capacitor for the output matching.

The choice of which matching network to use is generally a practical one. Notice, in this example, the first choice we made provides us with a convenient means of biasing the transistor without adding additional parasitics to the network other than the bypass capacitor. Another consideration might be the realizability of the elements. One configuration might give element values that are more realizable than the other.

Along these same lines, if the element values obtained in this process are too large, smaller values can generally be obtained by adding more circuit elements. But, as you can see, at the cost of added complexity.

In any case, our design example is essentially complete with the final circuit looking like this.

So far we have not considered noise figure in this design example. By plotting the noise figure circles for the device being used, we can readily determine the noise figure of the final circuit, which in this case is approximately 6 dB (Fig. 119).

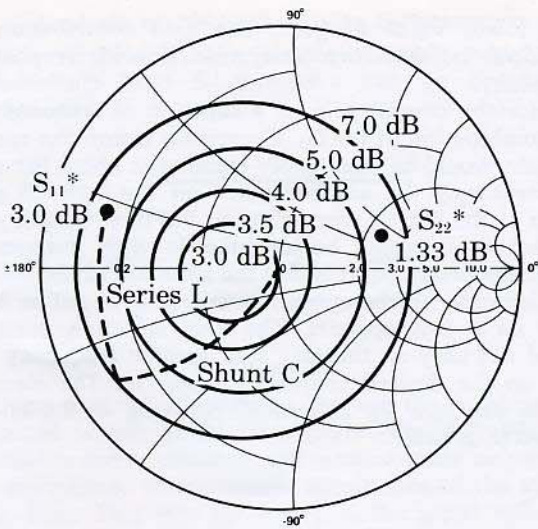


Figure 119

**B. Design for Minimum Noise Figure**

Let's now proceed with the second design example in which low noise figure is the design objective. This single stage amplifier will be designed to have minimum noise figure and 16 dB gain at 1 GHz (Fig. 120).

$$G_{Tn} = G_1 + G_0 + G_2$$

$$G_1 + 14 + G_2$$

$G_1$  and  $G_2$  are determined after input matching for minimum noise figure is accomplished

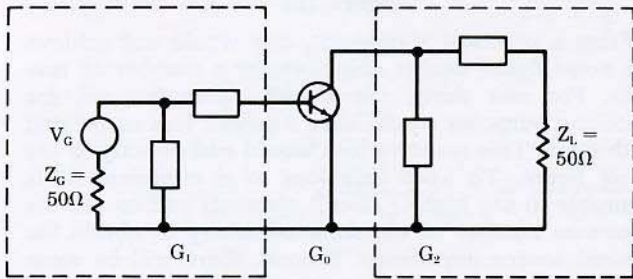


Figure 120

To accomplish the design, we first determine the input matching necessary to achieve minimum noise figure. Then using the constant gain circles,  $G_1$ , the gain contribution at the input can be determined. Knowing the gain of the device at 1 GHz, the desired value of  $G_2$ , the gain contribution of the output matching network, can then be found. The appropriate output matching network can be determined by using the constant gain circles for the output.

In this example a shunt capacitor and series inductor can be used to achieve the desired impedance for minimum noise figure. Referring once again to the Smith Chart and the mapping techniques used previously, we follow the constant conductance circle from the center of the Smith Chart and then proceed along a constant resistance circle (Fig. 121). Sometimes this requires several trials until the exact constant resistance circle that intersects the minimum noise figure point is found.

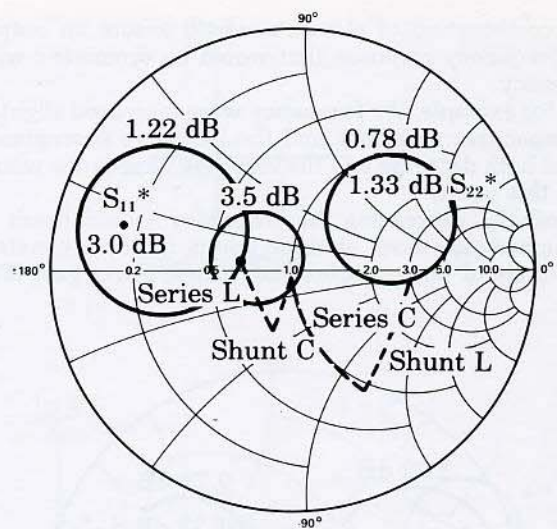


Figure 121

Since we now know that the minimum noise figure circle on the Smith Chart represents a specific source reflection coefficient, we can insert this value of  $\Gamma_s$  into the formula for  $G_1$  to determine the value of the input constant gain circle passing through this point. In this case, it is the 1.22 dB gain circle. This is 1.8 dB less than the maximum gain attainable by matching the input.

We can now calculate the output gain circle as follows. The desired gain is 16 dB. The gain due to the input matching networks is 1.22 dB and the forward gain of the device with 50-ohm source and load terminations is 14 dB. The gain desired from the matching network at the output is, therefore, 0.78 dB.

The output matching can again be accomplished by using a series capacitor with a shunt inductor. Notice that for the output matching there are an infinite number of points which would result in a gain of 0.78 dB. Essentially, any point on the 0.78 dB circle would give us the desired amount of gain.

There is, however, a unique feature about the combination of matching elements just selected. The value of capacitance was chosen such that this point fell on the constant conductance circle which passes through the maximum gain circle represented by  $S_{22}^*$  (Fig. 122).

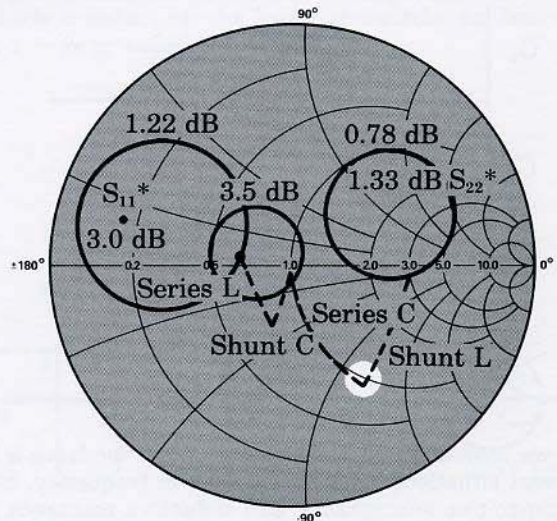


Figure 122

This combination of elements would assure an output gain-frequency response that would be symmetric with frequency.

If, for example, the frequency were increased slightly, the capacitive reactance and the inductive susceptance would both decrease and the resulting impedance would be at **this** point.

Similarly, decreasing the frequency would result in **this** impedance. Both of these points fall on a constant gain circle of larger radius and, hence, lower gain (Fig. 123).

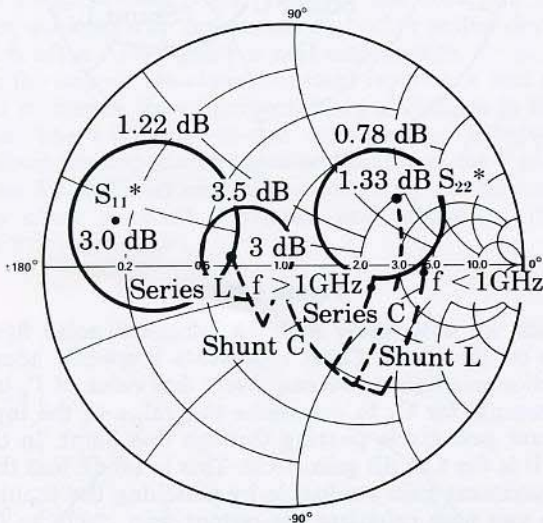


Figure 123

The gain response for the output matching, therefore, is more or less symmetric around the center frequency (Fig. 124).

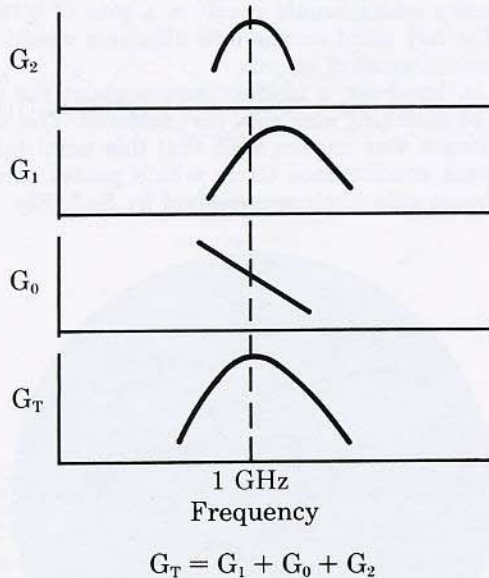


Figure 124

If we look at the input side, however, we have a far different situation. With an increase in frequency, both the capacitive susceptance and inductive reactance increase, resulting in an increase in gain. When the frequency is reduced, these quantities decrease, resulting

in a lower value of gain. The gain contribution at the input is, therefore, unsymmetric with respect to frequency.

Since the overall gain as a function of frequency is the combination of the  $G_1$ ,  $G_0$ , and  $G_2$  terms, the resulting gain would be reasonably symmetric about the center frequency. (If another point on the 0.78 dB gain circle at the output were chosen, the final overall gain characteristic would be **asymmetric** with frequency.)

The important point is that the selection of the matching elements for the output, in this case, is not as arbitrary as it first appears. The final selection must be based not only on the gain at a specific frequency but also on the desired frequency response. The element values can now be calculated resulting in the circuit shown (Fig. 125).

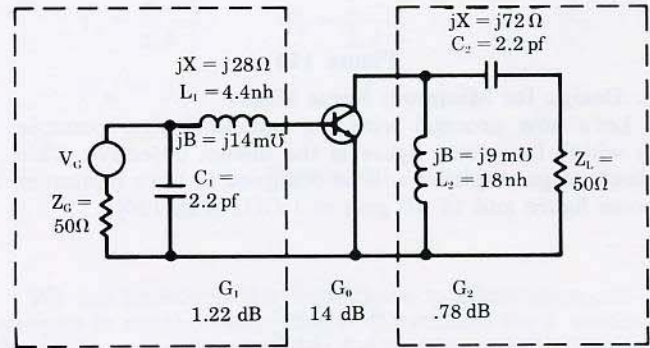


Figure 125

From a practical standpoint, one would not achieve the noise figure design objective for a number of reasons. For one thing, the circuit elements used for matching purposes would have a certain loss associated with them. This resistive loss would add directly to the noise figure. To keep this loss to a minimum, it is desirable to use high-Q circuit elements and to use the minimum number of elements necessary to obtain the desired source impedance. Second, there will be some contribution to the overall noise figure from the second stage. Third, additional degradation in noise figure would occur because of device and element variations from unit to unit.

In practice, typically  $\frac{1}{2}$  to 1 dB would be added from these sources to the predicted theoretical noise figure for a narrow band design. As much as 2 dB could be added in the case of an octave band design such as in our next example.

### C. Broadband Design for Specific Gain and Noise Figure

Here, the design objective will be 10 dB unilateral transducer gain from 1 to 2 GHz with a noise figure less than 4.5 dB (Fig. 126).

In this example, the input and output matching networks will be designed to have a gain of 10 dB at the band edges only. The gain at 1.5 GHz will then be calculated. The response will be found to look similar to this curve. If a greater degree of flatness were necessary, additional matching elements would have to be added. We could then design for 10 dB gain at three different frequencies, or more if necessary. Three frequencies would generally be the practical limit to the graphical design approach we have been using.

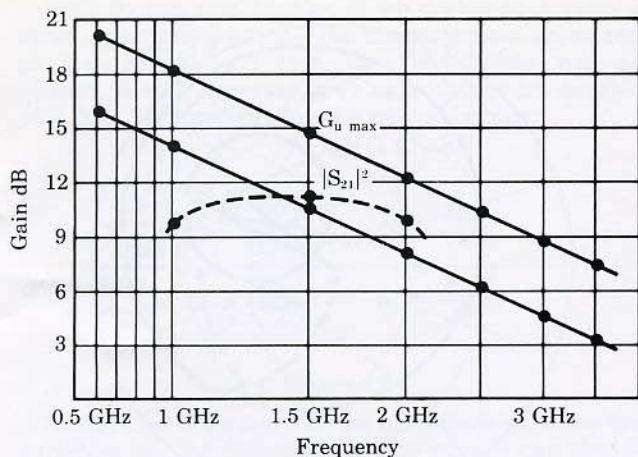


Figure 126

When matching is required at more than three frequencies, computer-aided design techniques are generally employed.

The schematic again looks similar to that which we had in the previous two examples (Fig. 127).

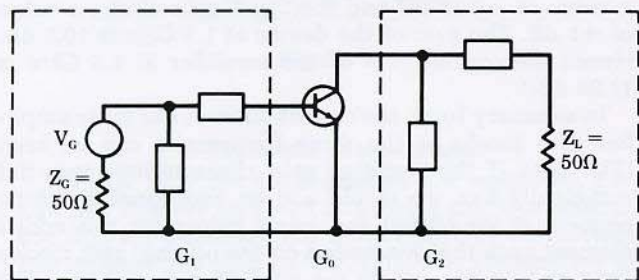


Figure 127

The design approach is to:

1. Match the input for the best compromise between low and high frequency noise figure. In this case, it is important to keep the number of matching elements to a minimum for the reasons cited earlier. It might be possible to get an additional 0.2 dB improvement in noise figure with one additional element, but the extra element might, in turn, add an additional insertion loss at 0.2 dB or more.
2. The next step is to determine the gain contribution at the input as a result of the noise figure matching. This then allows us to calculate the desired gain at the output from the design objective.
3. The output matching elements are then selected, completing the design.

Let's first plot  $S_{11}^*$  for 1 and 2 GHz and then plot the points resulting in minimum noise figure for these frequencies (Fig. 128).

<sup>1</sup> For the particular transistor measured. We want to emphasize that the methodology followed in these design examples is more important than the specific numbers.

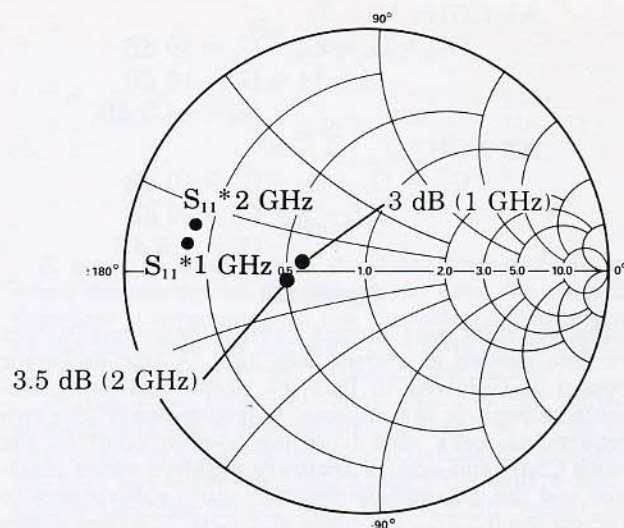


Figure 128

To match the input for minimum noise figure we must first choose a combination of elements which gives the best compromise at the two design frequencies. On the plot we see that a shunt capacitor followed by a series inductor will provide a source impedance such that the noise figure will be less than 3.5 dB at 1 GHz and less than 4.5 dB at 2 GHz<sup>1</sup> (Fig. 129). At both frequencies we are about as close as is practical to the theoretical minimum noise figure for the device.

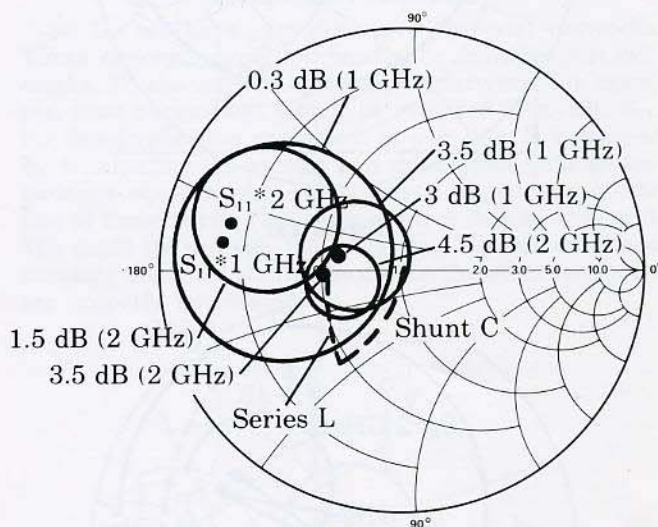


Figure 129

The constant gain circles, which intersect the points established by the input matching network, are calculated and found to have the values 0.3 dB at 1 GHz and 1.5 dB at 2 GHz.

The desired gain due to output matching can now be calculated and found to be  $-4.3$  dB at 1 GHz and  $+0.5$  dB at 2 GHz (Fig. 130).

AT 1 GHz

$$G_{Tu} = G_1 + G_0 + G_2 = 10 \text{ dB}$$

$$.3 + 14 + G_2 = 10 \text{ dB}$$

$$G_2 = -4.3 \text{ dB}$$

AT 2 GHz

$$G_{Tu} = G_1 + G_0 + G_2 = 10 \text{ dB}$$

$$1.5 + 8 + G_2 = 10 \text{ dB}$$

$$G_2 = +.5 \text{ dB}$$

Figure 130

The constant gain circles having these gain values are then plotted as shown (Fig. 131). A trial-and-error process is followed to find the proper matching elements to provide the required output match at the two frequencies. Let's start from the 50-ohm point on the Smith Chart and add an **arbitrary** negative series reactance and the appropriate negative shunt susceptance to land on the 0.5 dB gain circle at 2 GHz. We then determine where these matching elements will bring us at 1 GHz and, in this case, we fall short of reaching the proper gain circle (Fig. 132). By increasing the capacitive reactance we find a combination that lands on both circles and the design is complete (Fig. 133).

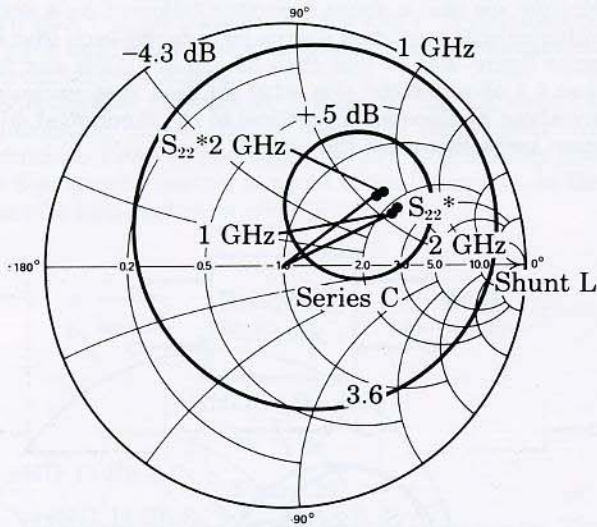


Figure 131

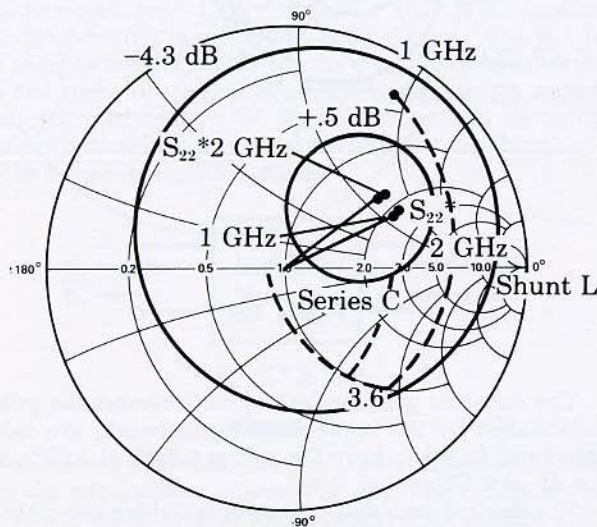


Figure 132

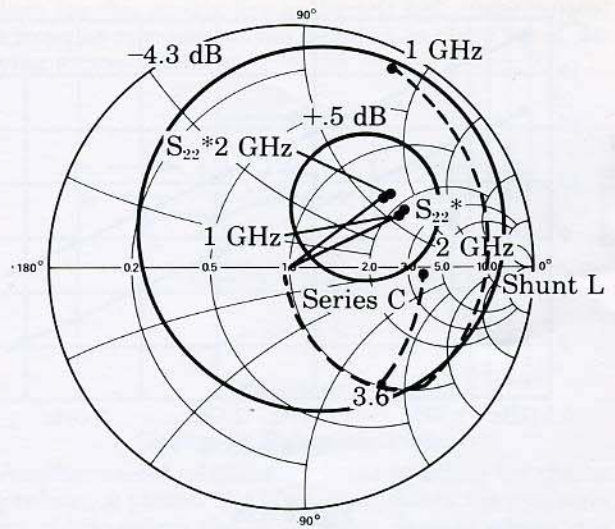


Figure 133

So far, by our design procedure we have forced the gain to be 10 dB at 1 and 2 GHz. The question naturally arises, what happens between these two frequencies? From the matching element values already determined, we can calculate the matching network impedances at 1.5 GHz and then determine the constant gain circles which intersect those points.

For this case, we find that the output gain circle has a value of  $-0.25 \text{ dB}$  and the input gain circle, a value of  $+1 \text{ dB}$ . The gain of the device at 1.5 GHz is 10.5 dB. Hence the overall gain of the amplifier at 1.5 GHz is 11.25 dB.

In summary form, the contribution of the three amplifier gain blocks at the three frequencies can be seen (Fig. 134). If the resulting gain characteristic was not sufficiently flat, we would add an additional matching element at the output and select values for this added element such that we landed on the original gain circles for 1 and 2 GHz, but on the  $-1.5 \text{ dB}$  rather than  $-0.25 \text{ dB}$  circle at 1.5 GHz. This would give us a gain for the amplifier of 10 dB at 1, 1.5, and 2 GHz with some ripple in between.

AT 1.0 GHz

$$G_1 + G_0 + G_2 = .3 + 14 - 4.3 = 10 \text{ dB}$$

AT 1.5 GHz

$$G_1 + G_0 + G_2 = 1.0 + 10.5 - .25 = 11.25 \text{ dB}$$

AT 2.0 GHz

$$G_1 + G_0 + G_2 = 1.5 + 8.0 + .5 = 10 \text{ dB}$$

Figure 134

If, however, we were satisfied with the first gain-frequency characteristic, our final schematic would look like this (Fig. 135).



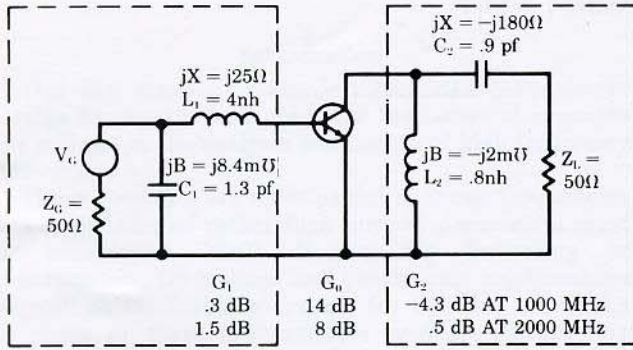


Figure 135

#### D. Multistage Design

While the examples we have just completed are single stage amplifiers, the techniques presented are equally applicable to multistage amplifier design. The difference in a multistage design is that the source and load impedances for a given stage of the amplifier are, in general, not 50 ohms but are rather an arbitrary complex impedance. In certain cases, this impedance might even have a negative real part.

Multistage design can be handled by simply shifting the reference impedance to the appropriate point on the Smith Chart. This is illustrated in the following example.

Let's now concentrate on the matching network design between two identical stages (Fig. 136). For the first stage, as we have seen, there is a gain of 1.3 dB attainable by matching the output to 50 ohms. Similarly, there is a gain of 3 dB attainable by matching 50 ohms to the input of the second stage. We can then think of a gain of 4.3 dB being attainable by matching the output impedance of the first stage to the input impedance of the second stage.

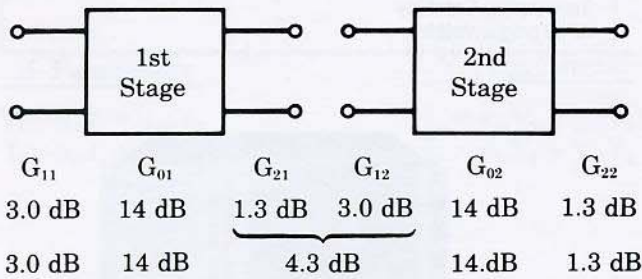


Figure 136

The constant gain circles for the first stage output would then be plotted on the Smith Chart (Fig. 137). The maximum gain is now 4.3 dB. The gain circle that intersects the point represented by the second stage's  $S_{11}$  has a value of 0 dB.

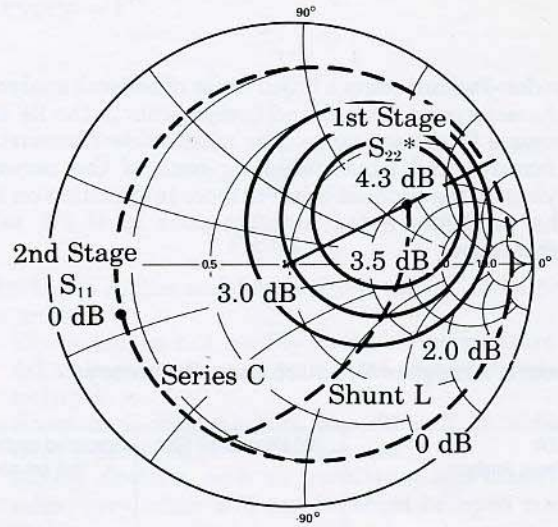


Figure 137

To design for a specific interstage gain, we could, as before, add a series capacitor followed by a shunt inductor—except in this case we start from the input impedance of the second stage,  $S_{11}$ , rather than the 50-ohm point.

The resulting interstage matching network looks like this. As you can see, the design of multistage amplifiers is as easily handled as single stage designs (Fig. 138).

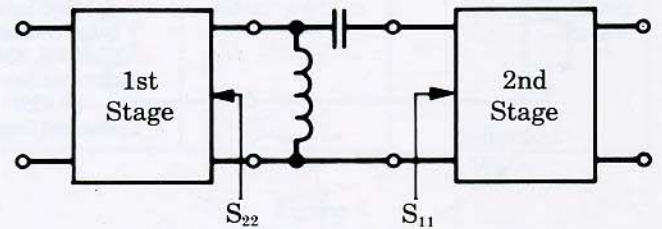


Figure 138

#### Summary

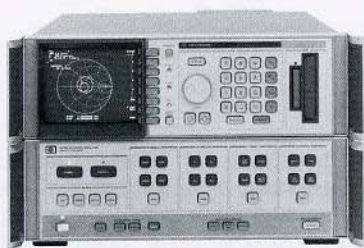
The measurement and design techniques demonstrated in this video-tape seminar are presently being used by engineers in advanced R&D labs throughout the world. When coupled with design and optimization computer programs, engineers will have at their disposal the most powerful and rapid design tools available.

## HP RF and Microwave Network Analyzers

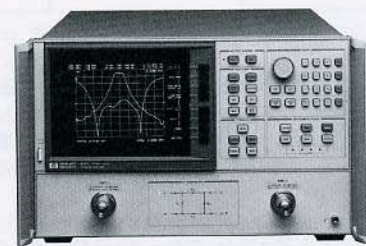
Hewlett-Packard offers a broad range of network analyzers for characterizing devices and components in the RF and microwave frequency range. The table below summarizes the features and capabilities for each of the network analyzers in the product line. For more information on any of the products listed, contact your local HP sales representative.

### Network Analyzer Product Line Summary

8752A Network Analyzer	300 kHz-1.3/3.0 GHz	Integrated synthesized source, test set and receiver	Transfer functions—magnitude/phase, insertion loss/gain, attenuation, gain compression, s-parameters, electrical length, group delay, deviation from linear phase. Impedance—magnitude/phase, return loss, r+jx accuracy enhancement time domain capability HP-IB programmable
8753B Network Analyzer	300 kHz-3 GHz/6 GHz	Integrated Synthesized Source	Transfer functions—magnitude/phase insertion loss/gain, attenuation, gain compression, s-parameters, electrical length, group delay, deviation from linear phase. Impedance—magnitude/phase—Return Loss, r+jx Full Accuracy Enhancement Time Domain Capability Harmonic Measurement Capability HP-IB programmable
8719A/8720B Network Analyzers	130 MHz-13.5 GHz (8719A) 130 MHz-20 GHz (8720B)	Integrated Synthesized Source (1 Hz Resolution Optional)	Transfer functions—magnitude/phase insertion loss/gain, attenuation, s-parameters, electrical length, group delay, deviation from linear phase. Impedance—magnitude/phase—Return Loss, r+jx Full Accuracy Enhancement Time Domain Capability HP-IB programmable
8510 Series Network Analyzer	45 MHz to 110 GHz	HP 8350 Series Sweep Oscillators HP 8340B, 8341B Synthesized Sweepers HP 8360 Synthesized Sweepers	Transmission/Reflection Characteristics S-parameters Active device characterization Full Accuracy Enhancement Time Domain Capability HP-IB programmable



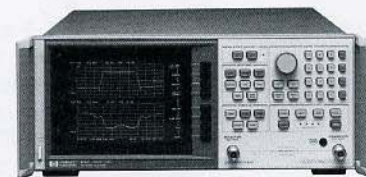
**HP 8510**  
Vector Network Analyzer



**HP 8720B**  
Economy MW Vector Network Analyzer



**HP 8753C**  
RF Vector Network Analyzer



**HP 8752A**  
RF Economy Vector Network Analyzer

# S-Parameter Design



**For more information, call your local HP sales office listed in your telephone directory or an HP regional office listed below for the location of your nearest sales office.**

**United States:**  
Hewlett-Packard Company  
4 Choke Cherry Road  
Rockville, MD 20850  
(301) 670 4300

Hewlett-Packard Company  
5201 Tollview Drive  
Rolling Meadows, IL 60008  
(708) 255 9800

Hewlett-Packard Company  
5161 Lankershim Blvd.  
No. Hollywood, CA 91601  
(818) 505 5600

Hewlett-Packard Company  
2015 South Park Place  
Atlanta, GA 30339  
(404) 955 1500

**Canada:**  
Hewlett-Packard Ltd.  
6877 Goreway Drive  
Mississauga, Ontario L4V 1M8  
(416) 678 9430

**Japan:**  
Yokogawa-Hewlett-Packard Ltd.  
15-7, Nishi Shinjuku 4 Chome  
Shinjuku-ku, Tokyo 160, Japan  
(03) 5371 1351

**Latin America:**  
Hewlett-Packard  
Latin American Region Headquarters  
Monte Pelvoux No. 111  
Lomas de Chapultepec  
11000 Mexico, D.F. Mexico  
(525) 202 0155

**Australia/New Zealand:**  
Hewlett-Packard Australia Ltd.  
31-41 Joseph Street  
Blackburn, Victoria 3130  
Melbourne, Australia  
(03) 895 2895

**Far East:**  
Hewlett-Packard Asia Ltd.  
22/F Bond Centre, West Tower  
89 Queensway, Central, Hong Kong  
8487777

**In Europe, please call your local HP sales office or representative:**

**Austria, COMECON-countries and Yugoslavia:**  
(0222) 2500 0

**Belgium and Luxembourg:**  
(02) 761 34 00

**Denmark:**  
(042) 81 66 40

**Finland:**  
(0) 88 721

**France:**  
(1) 60 77 42 52

**Germany:**  
(06172) 16 0

**Greece:**  
(01) 68 28 11

**Iceland:**  
(01) 671 000

**Ireland:**  
(01) 88 33 99

**Italy:**  
(02) 92 19 91

**Netherlands:**  
(020) 547 6669

**Norway:**  
(02) 24 60 90

**Spain:**  
900 123 123

**Sweden:**  
(08) 750 20 00

**Switzerland:**  
(057) 31 21 11 (Head office)  
(022) 780 41 11 (Suisse Romande)  
(046) 05 15 05 (Customer Information Center)

**U.K.:**  
(0734) 777 828

**Middle East and Africa:**  
Geneva-Switzerland  
41/22 780 7111

**European Headquarters:**  
Hewlett-Packard S.A.  
150, Route du Nant d'Avril  
1217 Meyrin 2  
Geneva-Switzerland  
41/22 780 8111